Copyright Warning & Restrictions

The copyright law of the United States (Title 17, United States Code) governs the making of photocopies or other reproductions of copyrighted material.

Under certain conditions specified in the law, libraries and archives are authorized to furnish a photocopy or other reproduction. One of these specified conditions is that the photocopy or reproduction is not to be "used for any purpose other than private study, scholarship, or research." If a, user makes a request for, or later uses, a photocopy or reproduction for purposes in excess of "fair use" that user may be liable for copyright infringement,

This institution reserves the right to refuse to accept a copying order if, in its judgment, fulfillment of the order would involve violation of copyright law.

Please Note: The author retains the copyright while the New Jersey Institute of Technology reserves the right to distribute this thesis or dissertation

Printing note: If you do not wish to print this page, then select "Pages from: first page # to: last page #" on the print dialog screen

Title of thesis : An Investigation of Electrical and Optical Properties of Reactively Sputtered Silicon Nitride and Amorphous Hydrogenated Silicon Thin Films

Tae Hoon Kim, Master of Science in Electrical Engineering, 1988

Thesis directed by : Dr. K.S. Sohn, Associate Professor of Electrical Engineering Department.

ABSTRACT

Thin films of silicon nitride and amorphous hydrogenated silicon were prepared by radio frequency reactive sputter deposition and their properties optimized for their use as low temperature passivation coatings for optoelectronic devices. The effect of various sputter deposition parameters on the conduction and optical properties were studied. Infrared spectrophotometry and ellipsometry were used to determined the optical properties of the films whereas the electrical properties were determined from current-voltage measurements of MIS capacitors.

Typical parameters of a sputter deposition run for the best Si_3N_4 films were : base pressure, $1\text{-}2x10^{-6}$ torr; sputtering pressure, 5 mtorr; nitrogen partial pressure,

16.5%; cathode anode gap, 10 cm; target power density, 1.97watts/cm^2; and cathode voltage, 1.9 kvolts. Films of thicknesses 50-120 nm, refractive index 1.94-2.2, and low conductivity (resistivity of $10^{11}\Omega$-cm) were obtained. The deposition rate was in the range of 5-8 nm/min depending on the sputtering pressure, the applied target power, and the nitrogen partial pressure. It was concluded that the quality of the silicon nitride films is strongly dependent on the total deposition pressure, nitrogen partial pressure, applied target power voltage, and possibly cathode voltage. It was also concluded that the water vapor background was the major factor in increasing the conductivity of the best films to values about three orders of magnitude above those for the best bulk silicon nitride material.

Typical sputtering parameters for depositing a-Si:H films were : base pressure, $1\text{-}2\text{x}10^{-6}$ torr; sputtering pressure, 7 mtorr; hydrogen partial pressure, 5-20%; cathode anode gap, 7.6 cm; r.f. target power density, 1.58-1.82 watts/cm^2; cathode voltage, 1.8-1.9 kvolts. Films of thicknesses 78-150 nm, refractive index 3.25-4.0, and strong absorption at 2000 cm^{-1} of infrared spectra were obtained. It was concluded that stoichiometric a-Si:H films can be prepared by reactive sputtering of a silicon target in the environment of argon and hydrogen.

AN INVESTIGATION OF ELECTRICAL AND OPTICAL PROPERTIES OF REACTIVELY SPUTTERED SILICON NITRIDE AND AMORPHOUS HYDROGENATED SILICON THIN FILMS

BY

TAE HOON KIM

Thesis submitted to the faculty of the graduate school of the New Jersey Institute of Technology in partial fulfillment of the requirements for the degree of Master of Science in Electrical Engineering

1988

APPROVAL SHEET

Title of Thesis : An Investigation of Electrical and Optical Properties of Reactively Sputtered Silicon Nitride and Amorphous Hydrogenated Silicon Thin Films

Name and degree : Tae Hoon Kim

Master of Science in Electrical Enginnering

1988

Thesis and abstract approved : _____

Dr. Kenneth S. Sohn
Associate Professor
Department of Electrical Engineering

Approval of faculty committee : _____

Dr. Roy H. Cornely
Professor
Department of Electrical Engineering

_____

Dr. Warren H. Ball
Graduate Associate Chairman
Department of Electrical Engineering

VITA

Name of candidate : Tae Hoon Kim

Permanent address :

Degree and date to be conferred : MSEE, May 1988

Date of birth :

Place of birth :

Secondary education : Sung Nam high school Korea

COLLEGIATE INSTITUTIONS ATTENDED	DATES	DEGREE
New Jersey Inst.of Tech., U.S.A.	1982-1986	BSEE
New Jersey Inst.of Tech., U.S.A.	1986-1988	MSEE

Major : Electrical Engineering

Positions held : Teaching Assistant 9/86 to 12/87
New Jersey Inst.of Tech., U.S.A.

Teaching Fellowship 1/88 to 5/88
New Jersey Inst.of Tech., U.S.A.

ACKNOWLEDGEMENTS

I would like to take this opportunity to express my sincere gratitute to Dr. Kenneth S. Sohn for his guidance and cooperation. Without his patience and support, I could have never done this research and thesis.

I would like to express my deep appreciation to Dr. Roy H. Cornely for providing technical advice and developing my interest in semiconductors.

I acknowledge the support from Mr.Raj Khandelwal for passing his experience with the sputtering system and making useful suggestions about the deposition experiments. I also acknowledge Mr.Diviang Shah for discussing and sharing the opinions about the results of the research experiment, and Mr.Gyuseok Kim for his invaluable assistance in helping conduct the sputter deposition run.

CONTENTS

LIST OF TABLES

LIST OF FIGURES

1 Introduction

Some of the research reported in this thesis was part of a research project on passivation of semiconductor surfaces. All the experiments were carried out under the supervision of Dr. K.S. Sohn and Dr. R.H. Cornely at Drexeler Microelectronics laboratories, Electrical Engineering Department, N.J.I.T., funded by an innovation partnership grant given by the New Jersey Commission on Science and Technology. The innovation partnership grant involved the New Jersey companies; Epitaxx Corp., Infrared Associates Inc., and Princeton Gamma Tech Corp.

The primary goals of this research were to develop a technology for passivating coatings of silicon nitride films and to prepare and characterize the amorphous hydrogenated silicon films. Passivating coatings are essential for a device to protect and improve its characteristics. They play a significant role in the device performance.

Si_3N_4 films are very important in semiconductor device fabrication because they afford a good moisture and contamination barrier.[1,2] Great effort has been made to investigate the formation and characterization of the film. For formation of Si_3N_4 films, Chemical Vapor Deposition (CVD) has most widely been in use. The method, however, has a disadvantage in regard to its high substrate temperature. To solve this drawback, a plasma-assisted CVD has been

recently developed [3,4]. This method uses a mixture of SiH_4 and NH_3 in the same manner as the CVD method. As a result, the silicon nitride films are contaminated with hydrogen, which degrades device characteristics.[5,6] However, in sputtering, films are deposited at low substrate temperature and are free from hydrogen contamination. These advantages make sputtering an attractive method to deposit Si_3N_4 films.

Thin insulating films of Si_3N_4 were made by reactive RF sputtering. There are various sputtering parameters such as RF power, distance between anode and cathode, ratio of partial pressure of argon and nitrogen gases, total gas pressure in the sputtering chamber and depositing time. In this thesis work, all parameters were set except RF power, total gas pressure in the sputtering chamber, ratio of partial pressure of argon and nitrogen. The settings of parameters, shown in table 1.1, were selected according to the results of previous research experiments in the Drexeler laboratory.

Anode Voltage	0 Volts
Distance	4 Inch
Presputter time	15 Min.
Depositing time	10 Min.

Table 1.1

The sputtering parameters were varied and a study of the effects of these parameters on the growth behavior of the films was conducted. The films' electrical and optical characteristics were also studied using Infra-Red Spectrophotometry, I-V measurements and ellipsometry. It was concluded that an attempt to make good insulating films of silicon nitride up to the level of reproducibility and possible usefulness as passivation coatings for optoelectronic devices was successful.

Thin films of amorphous hydrogenated silicon (a-Si:H) were also prepared by reactive RF sputtering. Hydrogenated amorphous silicon is a remarkable amorphous material showing high photoconductivity and efficient low temperature photoluminescence. While, the major device interests center at present around the potential use of a-Si:H as an inexpensive large-area solar cell, xerographic photoreceptor and thin film transistor, they possibly would be used as passivation coatings deposited at very low substrate temperature.

a-Si:H films are usually deposited by one of two methods: plasma-assisted decomposition of silane (glow-discharge technique) and cathodic sputtering of a silicon target in a mixture of argon and hydrogen. A generally observed trend is that glow-dicharge deposited films are of better quality than sputtered ones. This thesis work was concentrated on finding the optimized

preparation conditions for reactive sputtering. The ratio of the two reactant gases ,argon and hydrogen, and bias substrate voltage were the main deposition parameters investigated. The effect of the values of these parameters on optical absorption spectra and refractive index were studied.

The film deposition, characterization procedures, and the film properties obtained are discussed in detail in the various sections of this thesis. The following is a brief overview of each chapter.

The overview of various properties of Si_3N_4 and a-Si:H films is in chapter II. The properties of the films can be divided into mechanical, thermal, optical, electrical and chemical properties.

In chapter III, general techniques for characterizing the films are explained. The thickness of the films can be measured by mechanical, Ultra-Violet visible reflection spectra, and visible and Infra-Red radiation interference methods. The ellipsometric method can yield the film thickness as well as refractive index. The commonly used structural investigation methods are X-ray diffraction, electron diffraction, transmission electron microscopy, scanning electron microscopy and optical microscopy. Advantages and disadvantages of each technique, as well as the comparison among the techniques, were also presented in this chapter.

Chapter IV details the experimental procedure and techniques for preparation of the sputtered films. The description of the sputtering apparatus is also described in this chapter.

Experimental data and results obtained are presented in chapter V. A comprehensive discussion on the results is also presented in this chapter.

Finally, concluding remarks and suggestions for future work are presented in chapter VI.

II Overview of Various Properties of Si_3N_4 and a-Si:H Films.

2.1 Introduction.

This chapter presents various properties of Si_3N_4 and a-Si:H films. There have been a great deal of reports presenting various properties of Silicon Nitride and amorphous Hydrogenated Silicon in thin film form because of their high technological importance. The purpose of this overview is to outline all the properties which have been presented. The properties of films can be divided into mechanical, thermal, optical, electrical and chemical properties.

2.2 Mechanical and thermal properties.

The main mechanical and thermal properties of thin films are their adhesion to the support, their hardness and their thermal expansion coefficients.

The adhesion to the support is controlled by the nature of film support interaction forces (particulary forces of the van der Waals type or electrostatic forces). The adhesion also depends greatly on the nature of the support, on the cleanliness, microstructure and temperature, on the deposition process and on the subsequent treatment. As a general rule, good adhesion is obtained with a clean support which has few structural flaws and which is heated

at high temperature during the deposition process due to interdiffusion. However, this last condition leads to an increase in the number and intensity of mechanical stresses of thermal origin in the film. Subsequent heat treatment conducted in vacuo or in inert atmospheres improves the adhesion between the sample and the support. Adhesion can be qualitatively evaluated using a scratch test with a Talysurf diamond stylus. The stylus is moved while it is in contact with the sample and a lack of adherence is indicated by exposure of the silicon wafer along the track. Samples deposited at temperatures greater than 200°C pass this test.

Thin film microhardness can be measured using the Vickers or Knoop technique and a diamond indenter. The indenter (either a tetragonal or a rhombicpyramid) is dynamically applied, and the microhardness is determined by reading, with an optical microscope, the shape and magnitude of the indentation left on the film surface

Knoop microhardness values are estimated using the following relations:[7]

$$M_V = K_V P/d^2 \qquad P_V = d/7$$

or

$$M_K = K_K P/d^2 \qquad P_K = d/30.5$$

where M_V is the Vickers microhardness in kilograms per square millimeter, K_V is 1854.4, P is the load, d is the

diagonal of the square or rhombic trace, P_v (or P_K) is the depth of film penetration, M_k is the Knoop microhardness in kilograms per square millimeter and K_K is 14228.

The Knoop technique is preferred for thin films because of its lower penetration.

Films up to about 1 μm thick have a specular surface showing interference colors. For thicknesses greater than 1 μm the surface color becomes matte and the surface remains smooth.

Density determinations have been made by weighing the wafers on a semimicrobalance with and without the deposited Si_3N_4 and a-Si:H films, measuring the film thickness and the wafer diameter, and using the values thus found to compute the density value.

Mechanical stresses developed in thin films generally have two components: an intrinsic component which is characteristic of the layer and which is controlled by structural imperfections, impurities etc.

The stress may be positive or negative in sign, depending on whether an expansive or a compressive stress is developed within the layer.

It has been shown experimentally that the Knoop hardness of Si_3N_4 films deposited onto silicon varies from 2000 to 4500 kg mm^{-2} as a function of deposition process, where the Mohs hardness is 9.5 and the coefficient of thermal expansion is $4.2x10^{-6}$, which is higher than that for silicon

[8,9,10,11]. Si_3N_4 films deposited by CVD processes are under tensile stress whilst, those obtained by RF sputtering are under compressive stress.

2.3 Optical properties

Investigation into the optical properties [12,13,14,15,16] of thin Si_3N_4 and a-Si:H layers led to important conclusions about their structure, composition and physical-chemical properties. Among these optical properties, the most intensively investigated are the refractive index and the absorption and reflection of light.

In thin films, the refractive index can be established by three methods: interferometry, ellipsometry and a comparison between the deposited Si_3N_4 or a-Si:H film and certain oils whose refractive indices are known.

The refractive index can be determined by optical interference techniques. A smooth wedge is produced on a sample surface by removing part of the Si_3N_4 or a-Si:H film with HF. Half of the sample is then plated with a thin film of aluminium. An interferometer is used to measure the displacement of sodium light (λ = 5900 A°) interference fringes when the wedge in the metallized and in the non-metallized areas is crossed. Using the relations;

$d = p\lambda/2$ metallized area

and

$d = q\lambda/2(n-1)$ non-metallized area

the result $n = 1+q/p$ is obtained (where p and q are the fringe displacements over the metallized and non-metallized areas respectively, d is the film thickness and n is the refractive index).

The refractive index can also be determined by means of an ellipsometer with a mercury or laser light source.

When a beam of monochromatic light crosses a thin layer, the intensity of the light decreases as a result of reflection and absorption phenomena which take place in the layer. The dependence of the reflection coefficient on the frequency of the light used, or on its wavelength, is illustrated by the absorption spectrum under study.

The absorption spectra in the IR range are particularly important for Si_3N_4 and a-Si:H layers because they provide information on the molecular structure of the layers. Indeed, for Si_3N_4 the absorption peak due to the Si-N bond occurs at 11.5 μm, and for a-Si:H the absorption peak due to the Si-H bond occurs at 4.6 μm. Absorption peaks for Si-O (9.4μm), O-N (2.9μm), N-H (7.2μm) have seldom been found and are not observed in the data shown in Fig. 2.1 and Fig. 2.2. No shift in the absorption band was reported on high temperature annealing of the deposit.

2.4 Chemical properties

Si_3N_4 is highly resistant to many chemicals. However, it may be etched by fluoride solutions (either 48% HF and 52% distilled water or a mixture of 48% HF, 40% NH_4F and 12% distilled water), by non-fluoride solutions (85% H_3PO_4 refluxed) and by gaseous HCL according to the following reactions [17,18,19,20,21];

$$Si_3N_4 + 18HF = H_2SiF_6 + 2(NH_4)_2SiF_6$$
$$3Si_3N_4 + 27H_2O + 4H_3PO_4 = 4(NH_4)_3PO_4 + 9H_2SiO_3$$
$$Si_3N_4 + 16HCl = 3SiCl_4 + 4NH_4Cl$$

The dissolution rate of Si_3N_4 films is controlled by the film porosity (density), by the film stoichiometry, by bond strain and by impurities.

Semiconductor device technology often requires that certain preselected portions of Si_3N_4 films are etched; the portions to be preserved are masked by thin layers of either polycrystalline silicon (when using the 48% HF etch) or SiO_2 (when using the refluxed H_3PO_4 etch).

Plasma etching is a modern etching technique which is used for thin layers and is particularly successful for Si_3N_4. For Si_3N_4 films the plasma is obtained using RF discharges in a tetrafluoromethane-oxygen mixture. The etching rate is a function of the etching gas used, of the RF energy, of the etching gas flow rate and pressure, of the

amount and size of the wafers and of the distance between the wafers. For Si_3N_4 films the process of plasma etching is of the following form;

$$CF_4 \longrightarrow C+4F$$

$$O_2 \longrightarrow 2O$$

$$2Si_3N_4+5O+20F \longrightarrow 2SiF_4+2SiOF_2+Si_2OF_6+O_2+F_2+4N_2$$

The etching is caused by the oxygen and fluorine atoms in the plasma. Si_3N_4 reacts with the oxygen and the water only at high temperatures (1200 $^{\circ}C$) and at low rates [22]:

$$Si_3N_4+3O_2 \longrightarrow 3SiO_2+2N_2$$

$$Si_3N_4+6H_2O \longrightarrow 3SiO_2+4NH_3$$

Hence Si_3N_4 can be used as a masking material in the selective oxidation of silicon.

The high rate electrochemical oxidation [23,24] of Si_3N_4 takes place according to the following reaction:

$$Si_3N_4+6O^{2-} \longrightarrow 3SiO_2+2N_2+12e^-$$

The Si_3N_4 films are integrally converted into an SiO_2 film.

2.5 Electrical properties

Si_3N_4 films are electrical insulators.

Studies conducted on the electrical characteristics of Si_3N_4 films [25,26,27,28,29,30,31] have included the properties of the Si_3N_4-Si interface, the breakdown voltage, the dielectric constant and the electrical conductance.

The electrical characteristics of dielectric films are derived from studies of metal-insulator-semiconductor (MIS) capacitors where the metal is aluminium, gold or mercury, the insulators are SiO_2, Si_3N_4 etc. and the semiconductor is silicon. When the insulator is Si_3N_4, the capacitor is denoted by MNS. An MNS capacitor has two electrodes; one is connected to the metal deposited over the nitride and is called "the grid" and the other is represented by an ohmic contact to the semiconductor. The factors of interest are capacitance C between the two electrodes and its dependence on the d.c. voltage V_g applied to grid, *i.e.* the $C\text{-}V_g$ characteristic.

For an ideal MNS capacitance, the values of the capacitance are measured and plotted against the values of the voltage applied to the grid. A $C\text{-}V_g$ characteristic curve showing three areas-accumulation, depletion and inversion- is obtained.

The capacitance values of MNS devices varies from a maximum C_o to a minimum C_{min} according to the relation

$$\frac{C}{C_N} = 1 + \frac{2\,\varepsilon_N^{\,2}\,\varepsilon_o}{q\,N_A\,\varepsilon_{Si}\,X_N^{\,2}} V_g^{\,-1/2}$$

where C_N is the capacitance per unit area of nitride film, ε_N is the nitride dielectric constant, ε_o is the free space permittivity (8.86×10^{-14} F cm^{-1}), q is the electron charge (1.6×10^{-19} C), ε_{Si} is the silicon dielectric constant, N_A is the concentration of acceptor impurities, X_N is the thickness of the nitride layer and V_g is the grid voltage.

It can be seen that the capacitance value decreases with the square root of the grid voltage value. The real MNS capacitance shows a value for the work function difference which differs from zero and causes a horizontal shift of the $C-V_g$ characteristic.

At the same time, in an MNS capacitor the following mobile or fixed charges may exist causing a shift of the $C-V_g$ characteristic:

(1) Interface charges due to breaks in the semiconductor lattice at the interface.

(2) Fixed positive superficial charges near the Si_3N_4-Si interface, due to the non-stoichiometric Si:N ratio at the interface.

(3) Radiation charges, produced, for example, by cosmic radiation.

(4) Trapping charges of opposite polarity to those of the applied voltage develop in the Si_3N_4 layer from the silicon substrate.

(5) Ion charges (*e.g.* Na^+, K^+ and H^+), which have little

significance in an Si_3N_4 layer because of the blocking effect of this layer

(6) Dipole charges, due to dipole orientation after the applied voltage has induced a charge in the silicon.

Comparison of the experimental characteristic curve with the theoretical curve gives the voltage shift along the voltage axis, *i.e.* the flat band voltage V_{FB}. The flat band superficial charge (the amount of charge removed in order to bring the surface and the bulk to the same potential) is defined by the relation;

$$N_{FB} = C_N V_{FB}/q$$

where C_N is the capacitance value per square centimeter, V_{FB} is the flat band voltage, q is the electron charge and N_{FB} is the number of charges per square centimeter. The flat band voltage, and hence the flat band superficial charge, depends on time, temperature and bias values for capacitors measured in stressed conditions.

Si_3N_4 films serve to passivate the surface of silicon electrically, *i.e.* to maintain a constant potential difference between the surface and the bulk. This potential difference changes because of either charges, dipoles or ions present at or near the interface. The main drawbacks of an MNS structure are a high density of superficial charges and the existence of a trapping charge. To avoid

these hindrances , a metal-nitride-oxide-semiconductor (MNOS) device is preferred as it exhibits good electrical stability (the thermal oxide provides a low density of superficial charge and no interface trapping charge)(Table 2.1). A shift of the C-V_g characteristic could also be caused by the temperature or by the applied voltage. These electrical instabilities are explained by a redistribution of the insulator mobile charge. A shift of sign will depend on the sign of the potential bias applied on the grid. Trapping and dipole charge instabilities appear at high polarizing voltages V_p and during the bias temperature stress tests respectively. Superficial charges appear even at room temperature and at a low V_p (Fig. 2.3) Several techniques are applied to prevent instability of the C-V_g characteristic induced by mobile charges present in the insulator. One method consists of preventing ion contamination of the wafers. Another, which can be applied concomitant treatment which reduces the characteristic shift down to a few tenths of a volt under the action of temperature or/and of the electrical field.

$$\varepsilon = Cd/\varepsilon_o A$$

where C is the capacitance, d is the thickness of the Si_3N_4 layer, A is the capacitor area and ε_o is the free space dielectric permittivity. The value of the dielectric

system	Q_i	Q_f	Q_m	Q_r	Q_d	Q_t
Si_3N_4/Si	10^{12}	No	No	Yes	No	Yes
$Si_3N_4/SiO_2/Si$	10^{11}	Yes	Yes	Yes	No	No

Table 2.1

Electeric charges associated with the Si_3N_4/Si and $Si_3N_4/SiO_2/Si$ systems.

* Q_i, interface charges; Q_f, fixed surface charges; Q_m, mobile ion charges; Q_r, radiation charges; Q_d, dipole charges; Q_t, trapping charges.

constant varies from 5 to 9 depending on the technique used for the film preparation. If ε is known, then C can be measured and the thickness of the deposited the film can be estimated by computation.

The electrical conductance has been studied using the current-voltage relation [32,33,34,35,36]. The results obtained (Fig. 2.4) show that in general a non-linear relation of the form $\ln I \propto V^{1/2}$ exists. This dependence is explained by the fact that in Si_3N_4 films, the conduction mechanism does not obey Ohm's law; the Poole-Frenkel mechanism is obeyed, according to which thermal conduction takes place by means of either electrons or holes which are developed by thermal ionization of trapping levels in the

Si_3N_4 film and are stimulated by the electric field.

2.6 Applications

Deposits of Si_3N_4 thin films are widely used in semiconductors and in integrated circuit technology. Other applications include Si_3N_4 films on silicon, optical waveguides[37], and Si_3N_4 films for forming glass-to-metal seals.

Some of the many important applications of Si_3N_4 films are the following:

(1) electrical insulators, which have a comparatively high dielectric constant;

(2) chemically and electrically stable passivation layers for semiconductor surfaces, which withstand the corrosive action of most reagents and which prevent ion diffusion;

(3) and masks for semiconductors, to protect against donor and acceptor impurity diffusion (aluminium, boron, gallium, indium, arsenic, phosphorus, antimony, zinc etc.), as they are impermeable to these impurities under the normal diffusion conditions of p-n junctions.

Si_3N_4 films can be also be used for the following:

(1) as masks for semiconductors to protect against oxidation;

(2) as masks for selective epitaxial deposition of silicon[38];

(3) the storage of electric charges (memory effect)[39];

(4) the elimination of the effects of electric charges in SiO_2 to obtain devices with stable characteristics;

(5) decreasing the threshold voltage in insulated gate field effect transistors (FETs);

(6) and improving the high frequency performances of transistors.

Deposits of a-Si:H thin films are widely used in solar cell industry because of its high photoconductivity.

Amorphous hydrogenated silicon, a-Si:H, films can be used for the following:

(1) inexpensive large-area solar cell;

(2) xerographic photoreceptor;

(3) thin film transistors.

III. General Techniques for characterizing Films.

3.1 Film thickness and refractive index measurement

The thickness and refractive index of Si_3N_4 and a-Si:H films can be measured by mechanical, optical and electrical methods, *i.e.* the sample weighing method, the color chart method, the ellipsometric method, the method based on the use of UV-visible reflection spectra and the method based on visible or IR radiation interference.

3.1.1. Sample weighing method.

In this method, the support is weighed before and after deposition, and the film thickness can be determined if its density is known. The method can be useful for measuring the thickness even during layer deposition when, for example, the support is placed on one of the balance arms of a vacuum torsion balance.

3.1.2. Color chart method.

This method is based on the interference of visible radiation which has the same inclination to the wafer surface. If the direction of the incident radiation is nearly normal to the surface containing the film, and if the film is thin and uniform, then the whole film surface shows the same interference color. This color corresponds to a certain film thickness and it is impossible to determine the

thickness using a previous calibration, *e.g.* the table of interference color given in Table 3.1.

Si_3N_4 thickness (Å)	Si_3N_4 color
500	golden brown
1000	pale blue
1500	yellow
2000	dark red
2500	blue-green
3000	orange-yellow

Table 3.1

Color chart for selected Si_3N_4 film thickness

3.1.3. Ellipsometric method

In the ellipsometric method[48,49], modifications of the polarization state of a light wave, which are produced as a result of the interaction of the wave with the examined sample, are analysed. The polarization state is characterized by the phase and amplitude relations between the two plane waves which are components of the electric field vector in which the polarized oscillation can be solved. One wave p is in the incidence plane; the other wave s is normal to the incidence plane. The modification of the relative phases of the p and s waves is made by reflection. Reflection also modifies the amplitude ratio.

The ellipsometric magnitudes characteristic of the wave reflection on the sample surface are defined as follows: the angle Δ represents the phase modification and the angle ψ represents the factor by which the amplitude ratio is modified.

The ellipsometric data (the values Δ and ψ are determined experimentally) yield the refractive index and the film thickness when the fundamental relation of ellipsometry is applied:

$$\tan\psi \exp(i\Delta) = \frac{r_{1p} + r_{2p}\exp(-2i\delta) + r_{1s}r_{2s}\exp(-2i\delta)}{1 + r_{1p}r_{2p}\exp(-2i\delta)\; r_{1s} + r_{2s}\exp(-2i\delta)}$$

$$d = C_{n1}\delta$$

$$C_{n1} = (\lambda/2\pi)(n_1^2 - n_o^2 \sin^2\phi_o)^{-1/2}$$

$$d = (m\pi + x)\, C_{n1}$$

where d is the film thickness, δ is the phase difference, n_o is the refractive index of silicon. ϕ_o is the angle of incidence (70°), and r_1 and r_2 are the Fresnel reflection coefficients at the ambient-film and film-substrate interfaces respectively. The Fresnel reflection coefficients for reflection from the surface of a medium b into a medium a at the a-b interface are given by the fomulae:

$$r_p = \frac{n_a \cos \phi_b - n_b \cos \phi_a}{n_a \cos \phi_b + n_b \cos \phi_a}$$

$$r_s = \frac{n_a \cos \phi_a - n_b \cos \phi_b}{n_a \cos \phi_a + n_b \cos \phi_b}$$

A diagram (Fig.3.1) of the variation of Δ and ψ for different refractive indices n is obtained when the fundamental equation of ellipsometry is solved. The phase difference δ is also indicated in Fig.3.1. The thickness d is calculated by reading n_1 and δ from the graph (and evaluating m).

The ellipsometer is a special polarizing spectrometer(Fig.3.2) made up of the following parts: a monochromatic light source, a collimator, a polarizer which polarizes the light (Glan-Thompson prisms),a compensator (quarter-wave plate) which transforms the linearly polarized light into elliptically polarized light, a support on which the silicon sample covered with the Si_3N_4 and a-Si:H thin film is placed, an analyser and a detector.

In this method interference effects which appear in the layer-support systems are used to measure the film thickness. If the refractive index of the deposited material differs from the refractive index of the support, then the reflected light intensity is reduced to a minimum when the support-layer system is illuminated by

monochromatic light. The phenomenon is due to the extinction produced by interfernce of the reflected light with the free surface of the layer and with the support-layer interface. A series of maxima and minima are obtained.

There are two methods by which the interfernce fringes in the UV and visible reflection spectra can be obtained:

(1) the constant angle reflection interference spectrum (CARIS) method, in which the interference fringes in monochromatic light are observed as a function of wavelength at a constant angle of incidence;

(2) the variable angle monochromatic fringe observation (VAMFO) method, in which the interference fringes in monochromatic light are observed as a function of the angle of incidence at a constant wavelength.

The film thickness is given by

$$d = \frac{N \lambda_1 \lambda_2}{2(\lambda_1 - \lambda_2)(n^2 - \sin^2\phi)^{1/2}}$$

where ϕ is the angle of incidence, n is the film refractive index, λ_1 and λ_2 are two wavelengths corresponding to two interference maxima or minima values, and N is the number of interference fringes between the selected maxima or minima values. For the CARIS method, the measurement apparatus consists of a UV-visible spectrophotometer provided with a

reflectance attachment.

For the VAMFO method the light reflected by a silicon wafer covered with film is observed for different angles of incidence; the minima and maxima interferences are obtained as functions of the film thickness. The thickness is determined by a calibration procedure, *i.e.* by comparison with a known film thickness. The measuring apparatus for the VAMFO method consists of a fluorescent lamp, a mirror, a rotary support for the sample, a monochromatic filter and a microscope (Fig. 3.3).

3.1.5 Method based on visible or IR radiation interference

Recently a film thickness measurement method based on radiation interference has been proposed. The radiation can be emitted either by the substrate or by an external monochromatic source (*e.g.* a visible or IR laser). The interference curves (which appear as a result of multiple reflections between the Si-Si_3N_4 or Si-a-si:H and Si_3N_4-air or a-Si:H-air interfaces) are recorded and calibrated by measuring the thickness of the corresponding extremes using another method. The maxima and minima of the curve obtained correspond to constructive or destructive interference according to the relation $d = m\lambda/2n$, where d is the film thickness, m is the maximum or minimum order, λ is the radiation wavelength and n is the refractive index of the film. Enhancement of the light occurs when the film

thickness is an odd multiple of half the wavelength.

The deposition monitoring apparatus for the method based on the interference of visible or IR radiation emitted by the substrate (*e.g.* silicon) consists of a visible or IR radiation detector (optical pyrometer and IR pyrometer respectively) and a strip chart recorder.

The deposition monitoring system based on the observation of the visible or IR radiation intensity variation obtained from an external laser source shows some important advantages when compared with the previous system; it is possible to measure the thickness when deposition takes place at a temperature of 500°C and a better measurement accuracy can be obtained. However, this system requires more complex instrumentation; it contains the following component parts : a visible (or IR) laser placed outside the deposition chamber (the light of which is focused on the wafer where the thin layer will be deposited), a detector of the laser radiation reflected by the wafer, an amplifier, and a strip chart recorder (Fig. 3.4).

3.2 Measuring techniques for the structure of film

The study of film structure is particularly important when coupled with data concerning the film formation processes and with the physical-chemical properties of the films. For practical applications, it is equally important

to corelate structural properties with electrical, optical, mechanical, thermal, chemical and other film properties.

Methods applied to the study of the properties of thin films can be classified into those concerned with bulk investigation of the film throughout its whole depth and those concerned with investigation of the film surface only.

The main structural investigation methods are X-ray diffraction, electron diffraction, transmission electron microscopy (TEM), scanning electron microscopy(SEM) and optical microscopy.

3.2.1 X-ray diffraction

This is a highly accurate method of structural investigation and it offers many benefits over other methods. It requires very small amounts of sample, it requires little time to perform the measurement,and it is non-destructive. The X-ray diffraction interference patterns observed in crystals can be considered to be the result of interference radiation which is reflected by the various parallel planes in which the atoms of the crystalline lattice lie.

The condition for obtaining diffraction maxima is given by the Wulff-Bragg relation

$$2d \sin \theta = n\lambda$$

where d is the distance between crystallographic planes, θ is the angle of incidence, n is the reflection order and λ is the radiation wavelength. If λ and θ are known, then the distances d between reticular planes as well as the crystalline structure of the compound studied can be found. Tabulated values of the distances d for each crystalline compound allow the structures of the samples studied to be identified.

X-ray diffraction has shown that thin films of Si_3N_4 and Si:H deposited onto silicon are amorphous. To obtain crystalline films, either the film should be submitted to particle bombardment or the deposition process should take place at temperature higher than 1100°C in CVD method[40] .

3.2.2 Electron diffraction

Electron diffraction is one of the most favored techniques in the study of thin films. It offers some important advantages over X-ray diffraction, *e.g.* greater intensity of the diffraction lines and diffraction diagrams of very thin films can be obtained. The underlying principle of electron diffraction is the same as that for X-ray diffraction. For a crystalline sample an electron beam will be scattered at a variety of angles which all obey the Wulff-Bragg relation and diffraction spots can be recorded on a photographic plate.

The electron diffraction method, when applied to the

study of Si_3N_4 films, has led to the following results.

(1) Si_3N_4 films obtained by direct silicon nitridation are polycrystalline;

(2) Nitride and oxynitride films formed by CVD in the temperature range 700-1100°C yield images in the form of diffuse rings, which are characteristic of amorphous films;

(3) For Si_3N_4 films deposited using the RF glow discharge method the change in the intensity of the scattered electron beam as a function of the scattering angle can be used to derive the position, and the amount and type of atoms surounding a given atom (*e.g.* a silicon atom);

(4) The crystallite size and the nature (amorphous or crystalline) of Si_3N_4 films have been established.

3.2.3. Electron microscopy

Electron microscopy is widely used to obtain data on the morphology and structure of thin films. Techniques such as TEM, the replica technique, reflection microscopy and SEM are employed for the study of thin film structure.

Direct methods of electron microscopy rely on electron differential absorption in various regions of the sample, which causes image contrasts. Of course, owing to the strong electron absorption, TEM can only be applied to films up to a few ängströms in thickness. Consequently samples without supports are required. They can be obtained by chemical etching processes; essentially part of the

underlying support and, if necessary, even part of the film is etched away until the desired film thickness is reached.

The replica method is used extensively in the study of thin films, particularly when the films have been pyrolytically deposited. The resolution varies from 10 to 20 A and is limited by the grain size of the material used to produce the replicas.

In SEM the whole film surface is scanned by an electron beam and the image is given by the secondary electrons emitted by the sample. This technique has some important advantages over TEM; a) the surface of a comparatively bulky sample can be directly investigated; b) a wide field of investigation is available; c) a comparatively high resolution power is available.

Si_3N_4 films deposited onto silicon have been studied using TEM [41]. The samples were prepared either by thinning the silicon substrate through chemical etching or by using Pt-C replicas (carbon replicas shadowed with platinum). The results obtained show that the surface of the Si_3N_4 thin film varies as a function of the deposition conditions (the temperature, the SiH_4 concentration and diluent gas flow); smoother deposits result when the temperature and the SiH_4 concentration are low and when the diluent gas flow rate is comparatively high. SEM has been used successfully to detect growth flaws such as pinholes, inclusions and cracks in the films.

3.2.4. Optical microscopy

This method is used extensively to study the structure and morphology of thin films, and to obtain information about the film surface, the film topography, various types of flaws and the density of the film. Optical microscopes of the type employed in metallography are used with either polarized or unpolarized light in the visible, UV or IR ranges of the spectrum.

The main flaws found in the films are cracks in comparatively thick films deposited at a high rate or heat treated at high temperatures. These flaws are caused by strong interfacial stresses between the film and the silicon substrate; the stresses develop as a consequence of the difference in thermal expansion coefficients of the silicon and the films. Pinholes frequently develop in Si_3N_4 and a-Si:H films; they can be detected either by using etching solutions (*e.g.* a solution of ethylenediamine-pyrocatechol) or by an electrochemical method [42].

IV Experimental procedure and sputtering apparatus

4.1 Introduction

The sputtering apparatus is described and the experimental procedure is explained in this chapter. The old and new methods of chemical etching on silicon substrate are also presented.

4.2 Sputtering system

A modified version of MRC 8800 sputtering system was used for the deposition of Si_3N_4 and a-Si:H thin films. The method of sputtering involved Radio Frequency (RF) sputtering in diode and biased diode modes of operation. A schematic representation of the sputtering system is shown in Fig. 4.1. The RF generator, which operates at 13.56 MHz, supplies voltage to an intrinsic silicon target of 99.999% purity, 5.0 inch diameter and 0.25 inch thickness. The rotating target head can accomodate four targets fitted with ground shields. The substrates are laid on a 0.25 inch thick platen in the intervac chamber and then, are transported into the main chamber without breaking vacuum in main chamber. The distance between anode and cathode can be varied from 1.0 inch to maximum 4.0 inch. The main vacuum chamber is made of stainless steel. The stainless steel construction is preferred for the vacuum chamber because it absorbs relatively much less gas as compared to other

materials like glass, aluminium, etc.

The desired target could be positioned for sputtering by using the lever on the left hand side in the figure 4.1. The gases used for sputtering are supplied to the system through gas cylinders via a micrometering valve provided on the system. The most important parameter of the sputtering process is the vacuum pressure. To consider the vacuum low enough for sputtering, vacuum pressure has to be below 10^{-6} range.

The sputtering system has an intervac chamber. It is connected to the main chamber by a hinged-aluminium door. The samples are first placed in the intervac chamber. The intervac chamber is then pumped down to approximately 10 mtorr. The samples are then transported into the main chamber with a plunger. Thus the vacuum in the main chamber can be preserved.

4.3 Substrate and its chemical etching

4.3.1 Substrate

Silicon wafers were used as the substrates for the deposition of thin films of silicon nitride and amorphous hydrogenated silicon. The advantages of silicon as a a substrate for the experiments of this thesis were its low cost and its chemical stability.

N type, 2 inch diameter, single side polished, (1-1-1)

crystal orientation, 0.015 Ω-cm and 100 Ω-cm silicon wafers were used as substrates for the Si_3N_4 and a-Si:H film deposition. During each deposition run, both types of high and low resistivity silicon substrates were used. High resistivity substrates were used in the infrared absorption spectrum measurement. Low resistivity substrates were used for current-voltage measurement. (MIS devices were fabricated on the low resistivity substrates.)

4.3.2 Chemical etching of silicon substrates

Sample cleaning is very important for obtaining a good interface between the substrate and the film. Silicon substrates have a approximately 5-10 nm thick layer of native oxide which must be etched away before deposition.

The old procedure of sample cleaning is described below:

1) Chemically etch the substrate for 30 minutes in 49% Hydrofluoric acid (HF) under a venting hood.
2) Rinse in Methanol in two separate baths, rinse in 1,1,1 Trichloroethylene.
3) Finally rinse in two separate baths of Isopropanol.
4) Dry with helium or dry air blowing.

The above procedure has a problem of excessive chemical etching of the silicon substrates. Immersing silicon substrates for 30 minutes in 49% HF acid can damage the surface of silicon substrates. Therefore, a new sample cleaning procedure was adopted.

The new procedure is described below:

(1) Quickly dip the silicon substrates in 49% Hydrofluoric acid for chemical etching.

(2) Rinse in 1,1,1 Trichloroethylene.

(3) Rinse in two separate baths of Isopropanol.

(4) quickly dip one more time in 49% HF acid.

(5) Rinse in diluted water.

(6) Transport substrates to intervac immediately after drying the samples with helium or dry air.

4.4 Deposition process

The quality of films can be positively improved by reducing the contamination and improving the base vacuum pressure. To reduce the contamination, the vacuum chamber should be thoroughly cleaned. Since the vacuum chamber wall absorbs moisture from the atmosphere, it is desired that the chamber should not be opened and/or left open for longer durations than necessary.

To run the system, the vacuum of main chamber should be 1 to 2 x 10^{-6} torr. After the vacuum reaches the above range, the substrates were laid on the platen in the intervac chamber. The intervac chamber was then pumped down to approximately 10 mtorr. The substrate arrangement was drawn in the laboratory notebook for later reference during this pumped down duration. The sequence of operation is described below:

(1) The anode was lowered and the desired target was positioned to be sputtered.

(2) The intervac door was tripped to open and the plunger was moved in.

(3) The anode was raised to its upper limit when the plunger was all the way in.

(4) The plunger was retracted.

(5) The anode height was adjusted as desired.

After careful insertion of the substrates and the anode height adjustment, the stainless steel shield (presputtering shield) was used to cover the substrates.

The chamber was then evacuated for at least 2-3 hours before proceeding to actual deposition. The first step to actual deposition is admitting nitrogen or hydrogen gases to the main chamber up to a desired pressure through a micrometer leak valve. Argon gas was then introduced to the chamber and the total pressure was adjusted.

The purity of gases is very important for producing quality films. The desired purity of nitrogen gas and hydrogen gas is 99.999% and that of argon gas is 99.9995%.

Initially the total pressure was kept at $1-2x10^{-2}$ torr for igniting the plasma. Once the plasma was ignited, it was sustained at lower pressures. The pressure was quickly reduced to the desired value and the RF drive was adjusted to get the desired forward power. In any case, the reflected power should not exceed 75 watts, because high

reflected power could cause expensive as well as extensive damages to the RF generator.

The matching networks for the target were then tuned to obtain maximum forward power and minimum reflected power. After achieving the best tuning, all the parameters were precisely adjusted to the desired values with slight adjustments required in tuning. Special attention was given to forward power since it was directly related to the deposition rate.

The presputtering shield was removed only after the stable plasma was attained. This shield served several important functions such as preventing the deposition of sputtered material onto the substrates during the initial set up of plasma and presputtering the target. With the steady plasma and shield removed, deposition was carried out for the desired length of time and the sputtering parameters were noted down and verified after every 5 minutes.

The deposition parameters for a typical sputtering run were:

background pressure, $1\text{-}2\text{x}10^{-6}$ torr; total deposition pressure, 5-7 mtorr; anode to cathode distance, 4.0 inch; forward power, 200-240 watts; reverse power, 6-32 watts; cathode voltage, 1.3-1.9 kilo volts; anode voltage, 0 volts; and target power density 1.58-1.96 watts/cm^2 (target diameter, 12.7 cm).

For the fabrication of MIS capacitors, certain

substrates with Si_3N_4 film on them were selected for metallization. Aluminium was sputtered after masking the samples appropriately. For the metallization, it was generally observed that the aluminium film with the cathode voltage of more than 1.5 kvolt was a low quality film.

V Experimental Results and Discussion

5.1 Results and discussion of reactively sputtered amorphous Hydrogenated Silicon (a-Si:H) thin films

5.1.1 Introduction

Deposition conditions affect the film properties significantly and these properties can be varied in a controlled manner by controlling the deposition parameters. Among the deposition parameters, the effects of hydrogen partial pressure and bias sputtering on the film properties were investigated.

To characterize the films, infrared spectra, absorption coefficients, deposition rate and refractive index were measured and calculated. Experimental conditions and results obtained are presented at the end of this chapter.

5.1.2 Hydrogen partial pressure effect

5.1.2.1 Introduction

Although it has been reported that the incorporation of hydrogen eliminated states associated with dangling bonds from the pseudogap of the a-Si:H films [43], the precise manner in which the hydrogen modifies the material is not well understood, nor there is any consensus on just how much hydrogen is required to produce stoichiometric a-Si:H film.

It was previously found by other researchers that near stoichiometric a-Si:H films can be sputtered using the gas mixtures that vary between 10% and 50% of H_2. In my work, the best results as determined by I-R spectra and refractive index measurements were 10% H_2 and 90% Ar. The results are detailed in the next two sections.

5.1.2.2 Effect of hydrogen partial pressure on infrared transmission spectra - results and discussion

Associated with the Si-H bonds, three groups of spectral bands are observed: the Si-H bond stretch bands($\simeq$ 2000 cm^{-1}), the Si-H bond stretch bands ($\simeq$ 900 cm^{-1}), the Si-H bond wagging bands ($\simeq$ 600 cm^{-1}). Three spectra are shown in figure 5.1, 5.2, 5.3; the figures show the infrared transmittance of approximately 2500 Å thick films in the regions of Si-H bond stretching, bending, and wagging frequencies.

The infrared spectrum of sample ($R_7H\ S_3$) prepared in a gas mixture of 10% H_2 and 90% Ar is in figure 5.1. The spectrum shows strong absorption at the wave numbers of 2000 cm^{-1} and 600 cm^{-1}. The bending bonds at 900 cm^{-1} are extremely small, and are sometimes completely absent. This indicates that the films do not contain significant amounts of SiH_2 or $(SiH_2)_n$ groups. A similar result was observed by J. Tardy and R. Meaudre.[44]

The sample ($R_{11}H\ S_2$) was prepared in gas mixtures of

12% and 88% Ar, and its infrared spectrum is shown in figure 5.2. Compared with the data in Fig. 5.1, these data show only a small peak at 2000 cm^{-1}. The similar spectrum was obtained for films prepared in gas mixtures of 7-8% H_2 and 92-93% Ar.

Samples prepared in the gas mixture of more than 16% H_2 gave the infrared spectrum of figure 5.3. In the spectrum in this figure, there was no absorption caused by Si-H bonding. The peak at 1100 cm^{-1} is attributed to the Si-O stretching vibration.

Absorption coefficients were also calculated from the infrared spectra. To convert the transmittances to absorption coefficients, interference-free transmittance should be approximated by the general equation,

$$T = (1-R)^2 e^{-\alpha d} / (1-R^2 e^{-2\alpha d}) ,$$

where α is the absorption coefficient, d the film thickness, and R an empirically determined interface multiple reflection loss. Determining R by setting $T = T_o = 0.54$ when $\alpha = 0$, $T_o = 0.54$ is the theoretical as well as experimentally obtained Transmission.[45] Thus

$$T = \frac{4 T_o^2 e^{-\alpha d}}{(1+T_o)^2 - (1-T_o)^2 e^{-2\alpha}}$$

The absorption coefficients were calculated and plotted in figure 5.5.

The samples prepared in a gas mixture of 10% H_2 and 90% Ar gave the best results for infrared spectra. At low H_2 partial pressures, the films have more silicon and less hydrogen compared to stoichiometric a-Si:H. This explains the lower peak at 2000 cm^{-1} in Fig.5.2. As the % H_2 content increases, the film tends to become stoichiometric. At 10% H_2, the films were found to be stoichiometric and gave good absorption coefficients at the band for stretching.

5.1.2.3 Effect of hydrogen partial pressure on deposition rate - results and discussion

The deposition rate of the reactively sputtered amorphous Hydrogenated Silicon was found to be inversely proportional to the % H_2 content in the gas mixture of H_2 and Ar. This is explained by the difference of atomic weight of Ar and H_2. The atomic weight of H_2 is much smaller than that of argon. Because of this, argon has a larger sputtering yield than H_2. This explains the higher deposition rate at lower $\%H_2$ content in the gas mixture.

Figure 5.6 shows the plot of deposition rate versus $\%H_2$ at a total deposition pressure of 7 mtorr. At 10% H_2, the deposition rate was 57 Å/minute. With an increase in the % H_2 from 5% to 20%, the deposition rate dropped from 74 Å/min to 43 Å/min

5.1.2.4 Effect of hydrogen partial pressure on refractive index - results and discussion

The refractive index of bulk silicon is 4.05 at the wavelength of 5461 Å. At 10% H_2, the refractive index of a-Si:H was found to be 3.4. The refractive index of the a-Si:H thin film was reduced from 4.0 to 3.2 with a change in % H_2 from 5% to 20%. The refractive index of the perfectly stoichiometric amorphous hydrogenated silicon is reported in the literature to be around 3.4 [46].

Figure 5.7 shows the plot of refractive index versus $\%H_2$ at a total deposition pressure of 7 mtorr. There is an inverse relationship between the two of them. As the % H_2 content increases, the film tends to become stoichiometric which lowers the refractive index. With more than 10% H_2 in the gas mixture, however, the refractive index did not decrease rapidly.

5.1.3 Effect of substrate bias

5.1.3.1 Introduction

The influence of a negative substrate bias on the properties of reactively sputtered a-Si:H films has been investigated in this thesis work. Previously, Anderson, Moddel, Paesler and Paul [46] considered bombardment with energetic sputtered silicon atoms to be beneficial for the

film since the bombarding ions can remove loosely bound atoms on the surface of the growing film. This thesis work further investigated this phenomena.

5.1.3.2 Effect of substrate bias on infrared transmission spectra - results and discussion

Two spectra are shown in figure 5.1 and figure 5.4; the former is for an oxygen-free film, the latter for an oxygen contaminated film. In both cases, a peak at 2000 cm^{-1} is observed. The wagging-rocking band roughly centers at 600 cm^{-1}.

The dependence on bias voltage of the Si-H stretching bands at 2000 cm^{-1} is shown in figure 5.8. It was observed that the band at 2000 cm^{-1} depends very weakly on bias voltage. Figure 5.9 shows the strong dependence of the wagging band with bias voltage as the parameter. A net increase in the intensity of the band and a modification of its shape are seen as bias voltage increases. The mode at 600 cm^{-1} is largely affected by bias voltage.

As sputtered films always suffer negative ion bombardment, some defects due to this bombardment will be present in the film, although the extent of this damage is not kown at this time. Increasing the bias voltage causes a low-energy Ar^{+} surface bombardment, which improves both the surface mobility of adsorbed atoms and sputters poorly bound adsorbed species.

The results can be explained by considering two types of hydrogen-silicon bonding: isolated Si-H bonds, giving a mode at 2000 cm^{-1}, and clusters of Si-H bonds, giving a mode at 600 cm^{-1}. The results show that the mode at 600 cm^{-1} is certainly attributable to H atoms singly bound to Si atoms. The isolated bonds are known to be much stronger than the cluster bonds. Therefore, the results are consistent with the expectation that the weakly bound, cluster bonding, would be more affected by argon bombardment. This explains why modes at 600 cm^{-1} depend largely on the bias voltage.

The spectrum of Fig. 5.4 was recorded about two weeks after deposition and on samples kept at ambient atmospheric conditions. It is likely therefore that the films were contaminated by oxygen.

Figure 5.10 shows how the Si-O band decreases sharply as bias voltage increases. Figure 5.10 shows that the film contains large amount of oxygen for bias voltage less than 20 volts. A comparison of the spectra of Fig. 5.1 and Fig. 5.4 shows that a sharp decrease in the oxygen contamination for bias voltages in excess of about 40 volts.

The results can be explained by considering that if the substrate bias is zero or not sufficiently negative, no beneficial Ar^{+} bombardment occurs and less denses, less pure films might be obtained. The effective surface of the film is then larger and oxygen can penetrate deeply into the film and oxidize the inner surface. The bonding of oxygen atoms

with silicon weakens the Si-H bonding because of the difference in electronegativity. As the substrate bias increases, the density increases and the void regions are smaller and oxygen contamination can be reduced.

5.1.3.3 Effect of substrate bias on deposition rate

Figure 5.11 shows the inverse relationship between deposition rate and substrate bias. It can be seen that deposition rate depended on bias voltage. For 10% H_2 and zero bias voltage, the deposition rate was 57 Å/minute. For 10% H_2 and with a increasing bias voltage of 40 volts, the deposition rate dropped to 52 Å/minute. It also can be seen that the dependence on bias voltage increases as the % of H_2 decreases by comparing the curves of the 5%, 10% and 16% of H_2.

The result can be explained by considering that increasing the bias voltage allows low-energy Ar^+ surface bombardment. The low energy ion sputters away poorly bounded adsorbed species, and even host silicon atoms. This results in a lowering of the deposition rate.

5.2 Results and discussion of reactively sputtered silicon nitride (Si_3N_4) thin films

5.2.1 Introduction

Optical and electrical properties of reactively sputtered silicon nitride films were studied as a function of the following sputtering parameters: cathode voltage, nitrogen partial pressure and total depositing pressure.

Infrared spectrophotometry was used to analyse the influence of carrier gas on the composition of the films. It was observed that the properties of silicon nitride films were remarkably dependent on sputtering gas pressure. Results of conductivity measurement are discussed and also compared with the results presented in literature. This research experiment concentrated on finding the optimum preparation conditions to obtain low conductivity silicon nitride thin films.

The experimental parameters and their values are shown in table 5.3 on page 54.

5.2.2 Applied target power effect

Evidence was seen for an improvement of film quality at high target power. Such improvement can be explained in terms of energetic ion bombardment of the target, which result in the energy distribution of sputtered being shifted to higher energies.

The effect of target power on the deposition rate, refractive index, and I-R spectra was investigated.

5.2.2.1 Effect of applied target power on deposition rate

Figure 5.12 shows the dependence of the deposition rate on the applied target power. With increase in target power from 110 watts to 220 watts, the deposition rate increased from 55 Å/min to 83 Å/min. It can be seen that the deposition rate is directly proportional to the applied target power.

It should be noted that the cathode voltage unfortunately also changed since it was found that under the experimental conditions, it was difficult to keep the voltage constant while changing the applied target power. It was assumed that the dependence of film structure and stoichiometry was not a strong function of the cathode voltage. However, it is recognized that in future work, the dependence on the cathode voltage, with constant target power density and film deposition rate, ought to be studied. The possibility of negative ion bombardment of the substrate and the effect of changing energy of the sputtered atoms should be investigated.

5.2.2.2 Effect of applied target power on refractive index.

Figure 5.13 shows the dependence of refractive index on applied target power. With increase in applied target

power from 110 watts to 220 watts, the refractive index increased from 1.63 to 2.01. It was found that the films sputtered at low applied target power were non-stoichiometric under the partial pressure gas ratio used. The refractive index of the films tends to grow with higher applied target power, for the particular partial pressure gas ratio.

However, experiments to find the optimum gas pressure values for the lower cathode voltage were not done at this time. Changing the cathode voltage can result in a different altered layers in the silicon target surface, which requires a different nitrogen partial pressure to optimize the film stoichiometry. Also negative ions emitted from the target could play a role in resputtering the depositing film, preferentially sputtering nitrogen out of the film and creating defects and possibly voids.

5.2.3 Nitrogen partial pressure effect

It was observed that reactively sputtered silicon nitride films were stoichiometric or near stoichiometric at around 16% N_2 content in the gas mixture of Ar and N_2 in our sputtering system. With changing % N_2 content from 15% to 17%, the effects of nitrogen partial pressure on refractive index, I-V characteristic and infrared spectra of Si_3N_4 films were investigated.

5.2.3.1 Effect of nitrogen partial pressure on infrared spectra

Five spectra are shown in figure 5.14; all spectra exhibited broad classical Silicon Nitride absorption peak at approximately 840 cm^{-1}. Curve 5 is the best reported in literature[50]; it has large absorption peak at 840 cm^{-1} caused by Si-N stretching band. Curve 4 at a % Ar/N_2, 83.5/16.5 resembles the best published result. It can be seen that the % N_2 increases, the spectra has a larger absorption peak.

It was observed in a number of samples that there was broadening of the Si-N band near its baseline at 1200 $cm^{-1}$and shifting of the Si-N stretching band to lower wavenumbers. These results provide evidence that the amorphous Si-N absorption band appears to shift because of the presence of unwanted oxygen and hydrogen.

It is generally known that the presence of hydrogen deteriorates the physical and chemical properties of Silicon Nitride films. The presence of oxygen in the film is supposed to contribute towards higher conductivity in Si_3N_4 thin films.

The characteristic absorption bands for Si-O (centered at 1100 cm^{-1}), Si-H (centered at 880 cm^{-1}), and Si-N (centered at 840 cm^{-1}) are overlapped in the range of 800 to 1100 cm^{-1}. This increases the difficulties of analysing the infrared spectra of silicon nitride films.

5.2.3.2 Effect of nitrogen partial pressure on conduction mechanism - results and discussion

To study the conduction mechanisms in thin silicon nitride films, the dependence of current on applied capacitor voltage was measured for metal-insulator-silicon (MIS) capacitors, with about 800 Å insulator thickness. The dependences in terms of current density versus square root of electric field is plotted in Fig. 5.15; Curves 1 and 2 are the best results obtained in this work. They are for a nitrogen partial pressure of 16.5% with total pressures of 5 and 7 mtorr. Curves 3 and 4 are the best results reported in the literaure[50,51].

The least conducting films obtained in this thesis had higher conductivity by about three order of magnitude than in the literature. However, there was a improvement by a factor of two orders of magnitude during the course of this research. It was observed that the shape of the curve was similar to the reported work and therefore the conduction in the films was due to the Poole-Frenkel mechanism.

It was believed that the silicon nitride interface was not cleaned to satisfy scientific standards. By introducing a new cleaning procedure (explained in chapter IV), the film quality was improved. A comparison of the films under nearly the same conditions in table 5.3 shows that the films cleaned by using the former procedure were approximately one

or two orders more conducting than the films cleaned using the new procedure.

A possible explanation of the film's excess conductivity compared with the reported data of curve 3 and 4 is the incorporation of water vapor into the film structure during the deposition. This possible explanation is based on the results of the run performed after the surface of the chamber was heated for several hours, thus outgassed prior to the deposition; the films without heating the chamber prior to the deposition measured to be two or three orders more conducting than the films with heating the chamber prior to the deposition.

5.2.3.3 Effect of nitrogen partial pressure on refractive index

Table 5.1 shows that increasing nitrogen and argon partial pressure ratio, a decrease results in the refractive index. It can be observed that the refractive index and stoichiometry were very sensitive to the % N_2 in the total depositing pressure.

At low nitrogen partial pressure, insufficient nitrogen is available to form a silicon nitride on the film surface. This indicates that there are more silicon atoms and less nitrogen atoms on the film compared to stoichiometric silicon nitride films. The refractive indices of bulk silicon and silicon nitride are 4.05 and 2.1 respectively at

N_2/Ar % ratio	Refractive index
15/85	2.2
15.5/84.5	2.14
16/84	2.07
16.5/83.5	2.01
17/83	1.96

Table 5.1

Changes in refractive index with nitrogen/argon partial pressure ratio at total depositing pressure of 5 m torr.

the wavelength of 5461 Å. With increasing nitrogen partial pressure , the refractive index of the film tends to decrease.

It was found that stoichiometric Silicon Nitride films could be obtained at 16.5% N_2 content in the gas mixture of Ar and N_2 by reactive sputtering.

Exp. No.	Dep./Pre. Dep. Time (minutes)	Base Pressure x10 Torr	Deposition Pressure x10 Torr	Ar/H % Ratio	Anode Height (inch)	Cathode Voltage R.F. kV	Anode Bias R.F. kV	Forward Power (Watts)	Reverse Power (Watts)	Refractive Index	Film Thickness (A)	Deposition Rate (A/min)
1	20	1.8	7	95/5	3.0	1.9	0	220	12	4.0	1480	74
2	20	2.2	7	95/5	3.0	1.9	-21	200	8	3.98	1420	71
3	20	2.0	7	95/5	3.0	1.9	-38	210	8	3.95	1340	67
4	20	2.0	7	92/8	3.0	1.85	0	210	8	3.55	1260	63
5	20	2.1	7	92/8	3.0	1.9	-19	220	12	3.54	1220	61
6	20	2.0	7	92/8	3.0	1.85	-41	210	8	3.54	1160	58
7	20	2.0	7	90/10	3.0	1.9	0	220	12	3.4	1140	57
8	20	2.0	7	90/10	3.0	1.9	0	220	12	3.42	1132	56.6
9	20	2.0	7	90/10	3.0	1.9	-22	210	10	3.41	1100	55
10	20	2.0	7	90/10	3.0	1.85	-42	210	8	3.40	1040	52
11	20	1.5	7	88/12	3.0	1.9	0	230	14	3.3	1040	52
12	20	2.2	7	88/12	3.0	1.9	-18	210	8	3.32	1000	50
13	20	2.2	7	88/12	3.0	1.85	-41	210	10	3.33	945	47.3
14	20	1.8	7	86/14	3.0	1.9	0	230	14	3.25	960	48
15	20	2.1	7	86/14	3.0	1.85	-22	220	10	3.26	921	46
16	20	2.0	7	86/14	3.0	1.9	-43	220	12	3.28	863	43
17	20	2.1	7	84/16	3.0	1.9	0	220	12	3.22	906	45
18	20	2.2	7	84/16	3.0	1.9	-21	210	6	3.24	866	43
19	20	2.1	7	84/16	3.0	1.85	-42	220	8	3.25	816	41
20	20	1.9	7	80/20	3.0	1.9	0	220	12	3.21	862	43
21	20	1.7	7	80/20	3.0	1.85	-20	210	8	3.23	831	41.5
22	20	1.8	7	80/20	3.0	1.9	-41	220	12	3.25	781	39

Table 5.2

Results and sputtering conditions of a-Si:H films

Exp. No.	Dep./Pre. Dep.Time (Minutes)	Base Pressure $x10^{-6}$ Torr	Deposition Pressure $x10^{-3}$ Torr	N_2/Ar % Ratio N_2/Ar	Anode Height (inch)	Cathode Voltage R.F. kV	Anode Bias R.F. kV	Forward Power (watts)	Reverse Power (watts)	Refractive Index	Film Thickness (Å)	Deposition Rate (Å/min)
1	10	2	5	15/85	4	1.9	0	220	8	2.2	830	83
2	10	1.8	5	15.5/84.5	4	1.9	0	220	12	2.14	838	84
3	10	2.2	5	16/84	4	1.9	0	230	14	2.07	829	83
4	10	2	5	16.5/83.5	4	1.9	0	220	8	2.01	832	83
5	10	2	5	17/83	4	1.9	0	220	10	1.97	840	84
6	10	2.1	5	16.5/83.5	4	1.7	0	180	12	1.98	814	81
7	10	2	5	16.5/83.5	4	1.5	0	130	12	1.74	648	65
8	10	2	5	16.5/83.5	4	1.3	0	110	10	1.63	546	55
9	10	1.8	6	15/85	4	1.9	0	220	8	2.36	812	81
10	10	2.1	6	15.5/84.5	4	1.9	0	220	12	2.30	808	81
11	10	2.0	6	16/84	4	1.9	0	220	12	2.22	806	81
12	10	2.0	6	16.5/83.5	4	1.9	0	220	12	2.17	807	81
13	10	2.9	6	17/83	4	1.9	0	230	16	2.12	800	80
14	10	2.8	6	16.5/83.5	4	1.7	0	170	12	2.10	778	78
15	10	2.2	6	16.5/83.5	4	1.5	0	130	10	1.81	616	62
16	10	2.0	6	16.5/83.5	4	1.3	0	100	12	1.59	521	52
17	10	2.1	7	15/85	4	1.9	0	220	12	2.18	784	78
18	10	2.4	7	15.5/84.5	4	1.9	0	220	12	2.13	780	78
19	10	2.0	7	16/84	4	1.9	0	220	12	2.05	772	77
20	10	2.4	7	16.5/83.5	4	1.9	0	220	12	2.00	768	77
21	10	2.8	7	17/83	4	1.9	0	230	18	1.96	775	78
22	10	2.6	7	16.5/83.5	4	1.7	0	180	12	1.94	742	74
23	10	2.2	7	16.5/83.5	4	1.5	0	140	10	1.68	602	60
24	10	2.4	7	16.5/83.5	4	1.3	0	110	12	1.54	508	50

Table 5.3

Results and sputtering conditions of Silicon Nitride films

VI Conclusions and suggestion for future work

6.1 Conclusions

Sputtered Silicon Nitride films were studied using ellipsometry, infrared spectrophotometry and conductivity measurements. From the analysis of the results, it was concluded that low conductivity films of Si_3N_4 can be prepared by reactive sputtering of silicon target in a gas mixture of argon and nitrogen. Resistivity of $10^{11}\Omega$-cm were obtained and the results indicate that even lower conducting films can be prepared by installing a nitrogen trap for water vapor in the sputtering chamber and by further optimization of depsiting parameters.

It was found that near stoichiometric Si_3N_4 films can be obtained with a base vacuum pressure of $1\text{-}2\text{x}10^{-6}$torr; cathode voltage of more than 1.7 kV; % N_2/Ar, 16.5/83.5; sputtering pressure , 5-7 m torr; forward power, 200-230 watts; reflected power, 6-13 watts; and target power density, 1.58-1.96 watts/cm^2.

Stoichiometric Si_3N_4 films are characterized by strong infrared absorption at 840 cm^{-1}, a refractive index of 2.01, and high resistivity with a Frenkel-Poole J versus E conduction behavior.

It was found that the film quality depends strongly on the nitrogen partial pressure and the applied target power, and possibly also on cathode voltage. The film's refractive

index, I-R spectra, and conductivity were found to be very sensitive to the partial pressure of nitrogen.

Although the films with refractive index of 2.01 could be obtained repeatedly, the films with low conductivity could not be produced repeatedly. Conductivity of a film is greatly affected by the impurities and other defects in the film. Changes in the cleanliness of the substrate surface and the background water vapor partial pressure are believed to have been the main factors causing the variation in film conductivity. Water vapor is a paricular suspect since there was large drop in film conductivity when the chamber wall was heated prior to sputter deposition. Unfortunately, the residual gas analysis equipment was not operating when the experiments were made.

Introduction of a new substrate cleaning procedure significantly reduced the conductivity of the films. The best films were still three orders more conducting than the best published results for reactively sputtered thin films [51].

For the same gas pressure and same target power density, the effect of the cathode voltage should be studied to observe if conductivity and the density of defects in the sputtered films are related to negative ions emitted from the target, and also to see if changing the energy of the sputtered atoms effects the film properties.

Sputtered amorphous hydrogenated silicon films were

also prepared and studied. It was found that nearly stoichiometric a-Si:H films could be produced with a base pressure of $1-2x10^{-6}$ torr; depositing pressure of 7 mtorr; cathode voltage, 1.8-1.9 kvolts; $\%H_2/Ar$, 10/90; forward power, 210-230 watts; reflected power, 6-12.5 watts; and target power density, 1.58-1.96 watts/cm^2. It was found that the film's refractive index and I-R spectra were strongly dependent on hydrogen partial pressure. It was also found that an r.f. substrate bias of 40 volts greatly reduced the oxygen contamination in the film, as determined from the I-R spectra. An r.f. bias of 20 volts had little effect on the oxygen contamination in the film.

It was concluded that stoichiometric a-Si:H films can be prepared by reactive sputtering of a silicon target in the environment of argon and hydrogen using the Drexler laboratory sputtering system. These films are of sufficiently high quality to be used to investigate the application of amorphous hydrogenated silicon films as passivation coatings for three-five compound optoelectronic devices.

6.2 Suggested future work for silicon nitride

The following suggestions for future silicon nitride research are suggested by the author:

(1) Residual gas analysis should be used to analyse the gas contents in the sputtering chamber;

(2) A liquid nitrogen trap should be installed in the sputtering chamber to reduce water vapor residual background, which is known to increase the conductivity of the film;

(3) Substrate temperature should be controlled and the conductivity of the film should be studied as a function of substrate temperature;

(4) The effect of various substrate cleaning procedures on conductivity should be studied;

(5) Study of film properties versus cathode voltage with fixed deposition rate, applied power, and gas partial pressures should be done. The triode mode, which enables the target voltage to be as low as 100 volts, should be used to see if secondary negative ions and electrons are having any effect on the film properties;

(6) The effect of negative bias, as a mean of removing incorporated impurities, should be studied.

6.3 Suggested future work for amorphous hydrogenated silicon

The following suggestions for further improving the insulating properties of sputtered amorphous hydrogenated silicon thin films are given:

(1) A liquid nitrogen Meissner trap should be installed in the sputtering chamber to reduce water vapor residual background, which is known to reduce the minority carrier

lifetime causing recombination in the space-charge region[48].

(2) a-Si:H film is widely used as a solar cell. Therefore, it would be interesting to measure the photoconductivity of the films.

(3) A schottky barrier structure of a-Si:H could be prepared and the efficiency of the solar cell structure could be studied.

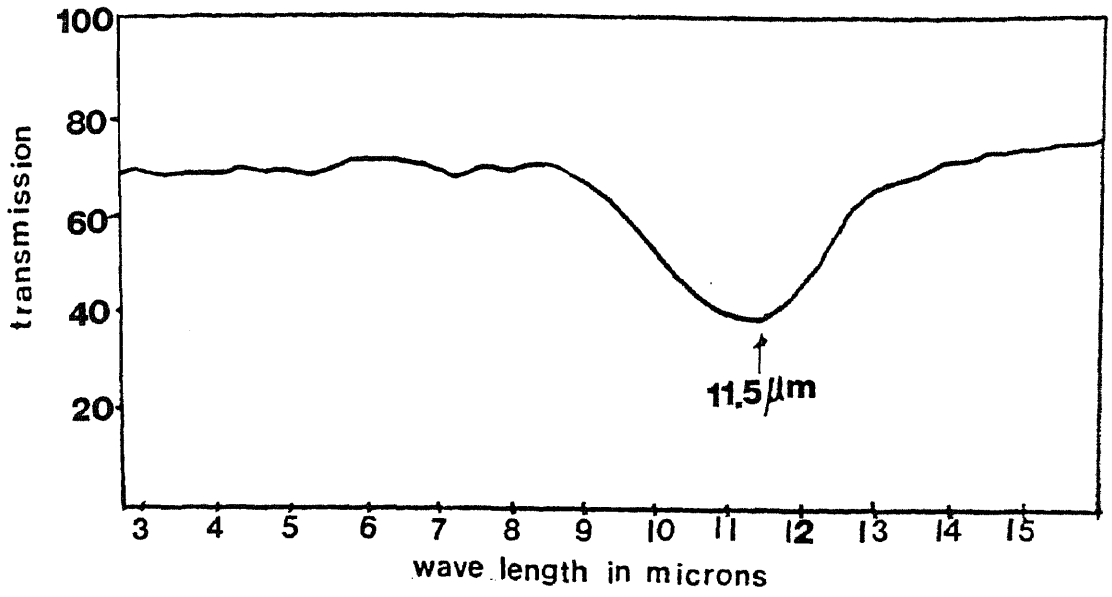

Fig.2.1 A typical IR transmission spectrum of an Si_3N_4 film.

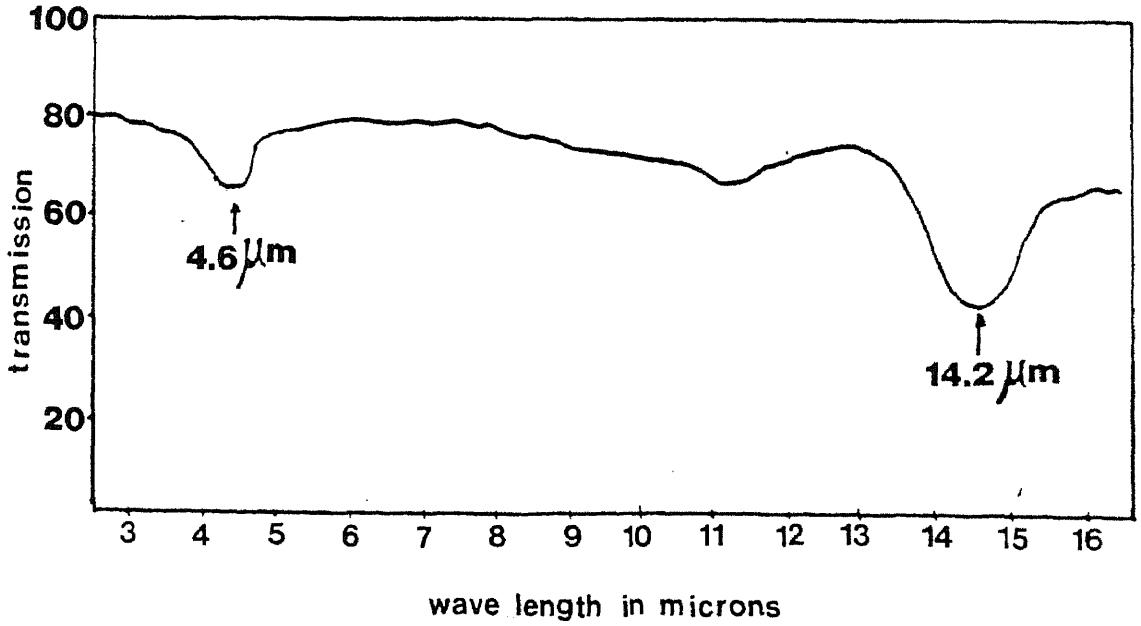

Fig.2.2 A typical IR transmission spectrum of an a-Si:H film

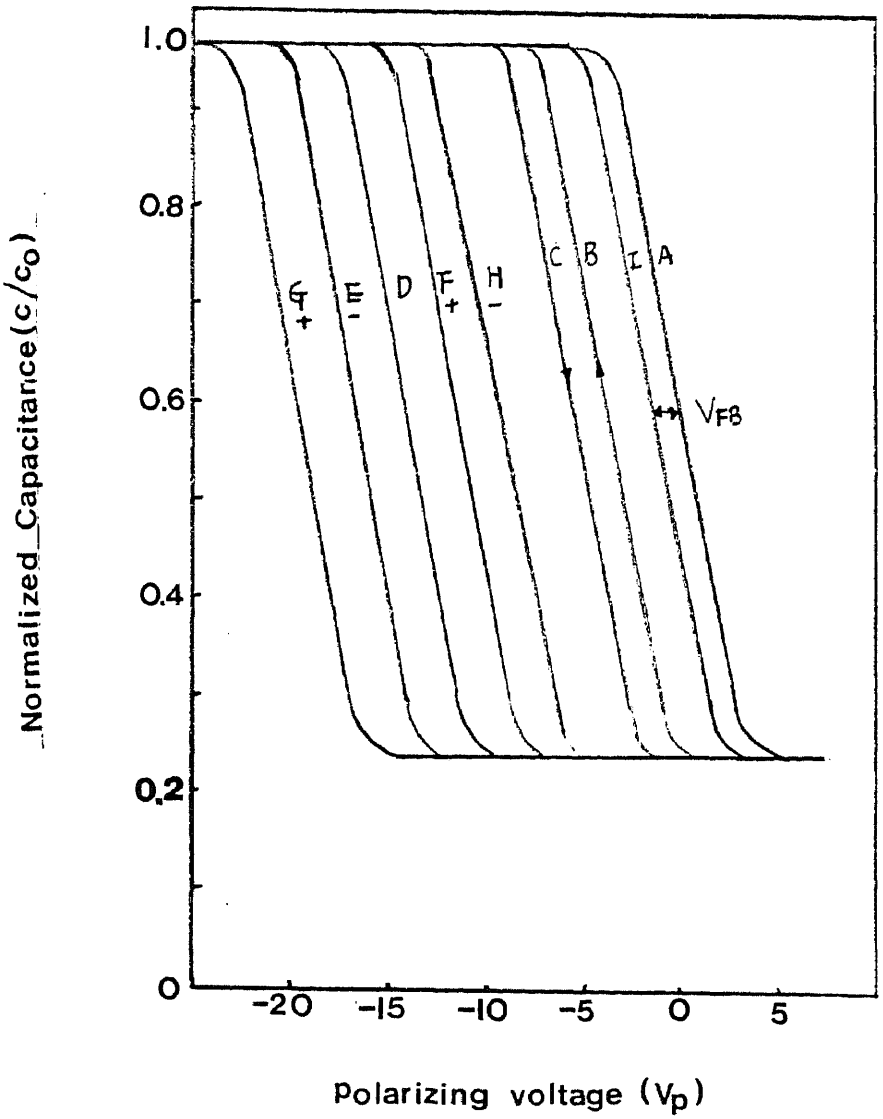

Fig 2.3. Typical capacitance-voltage curves for an MNS capacitor: A, theoretical curve; B,C, curves showing hysteresis of an MNS capacitor; D, curve for an MNS capacitor as deposited; E,F, curves for an MNS capacitor subjected to high negative and high positive polarizing voltages; G,H, curves for an MNS capacitor after a bias-temperature stress test; I, for an MNOS capacitor.

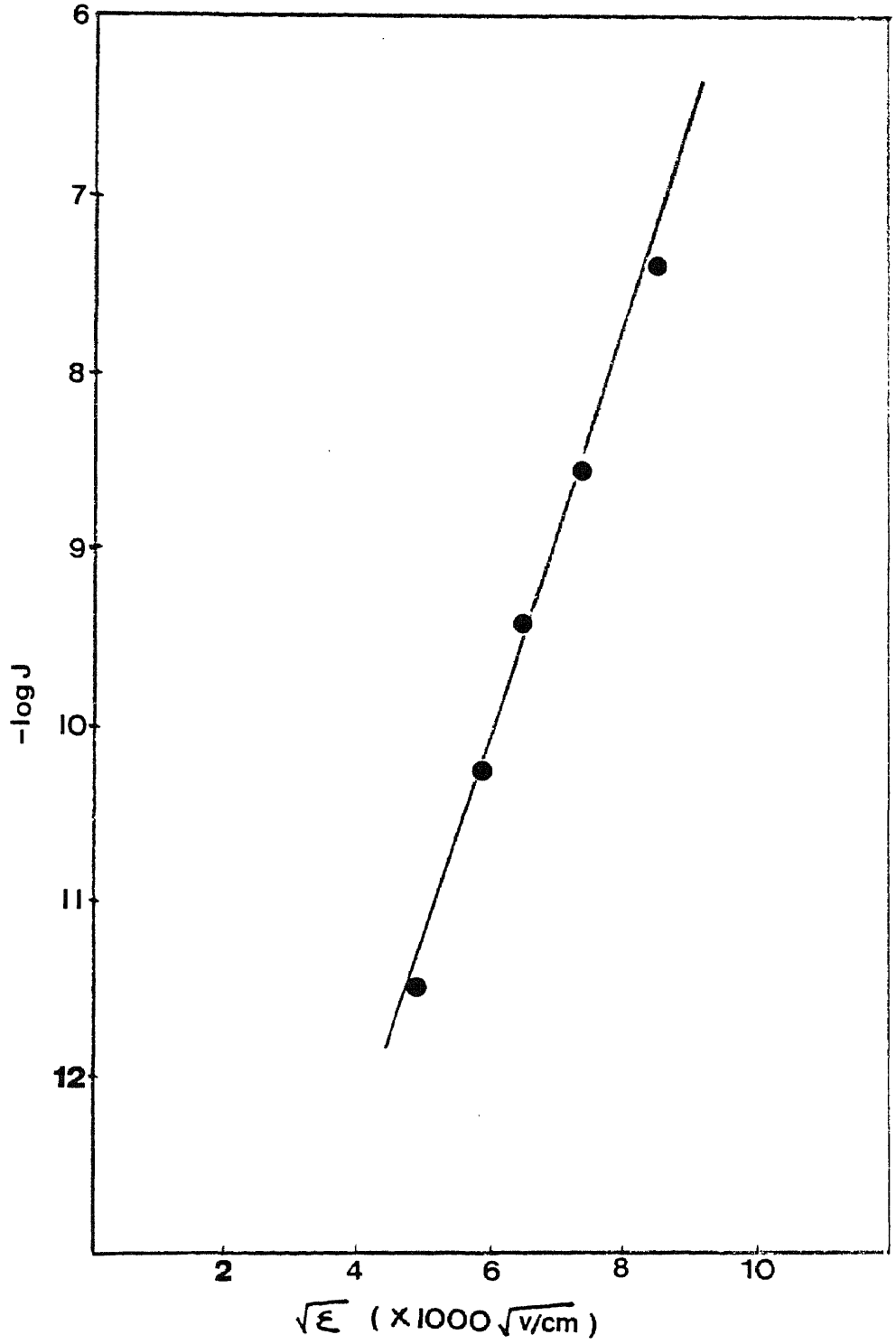

Fig. 2.4

A typical current-voltage curve for an MNS capacitor

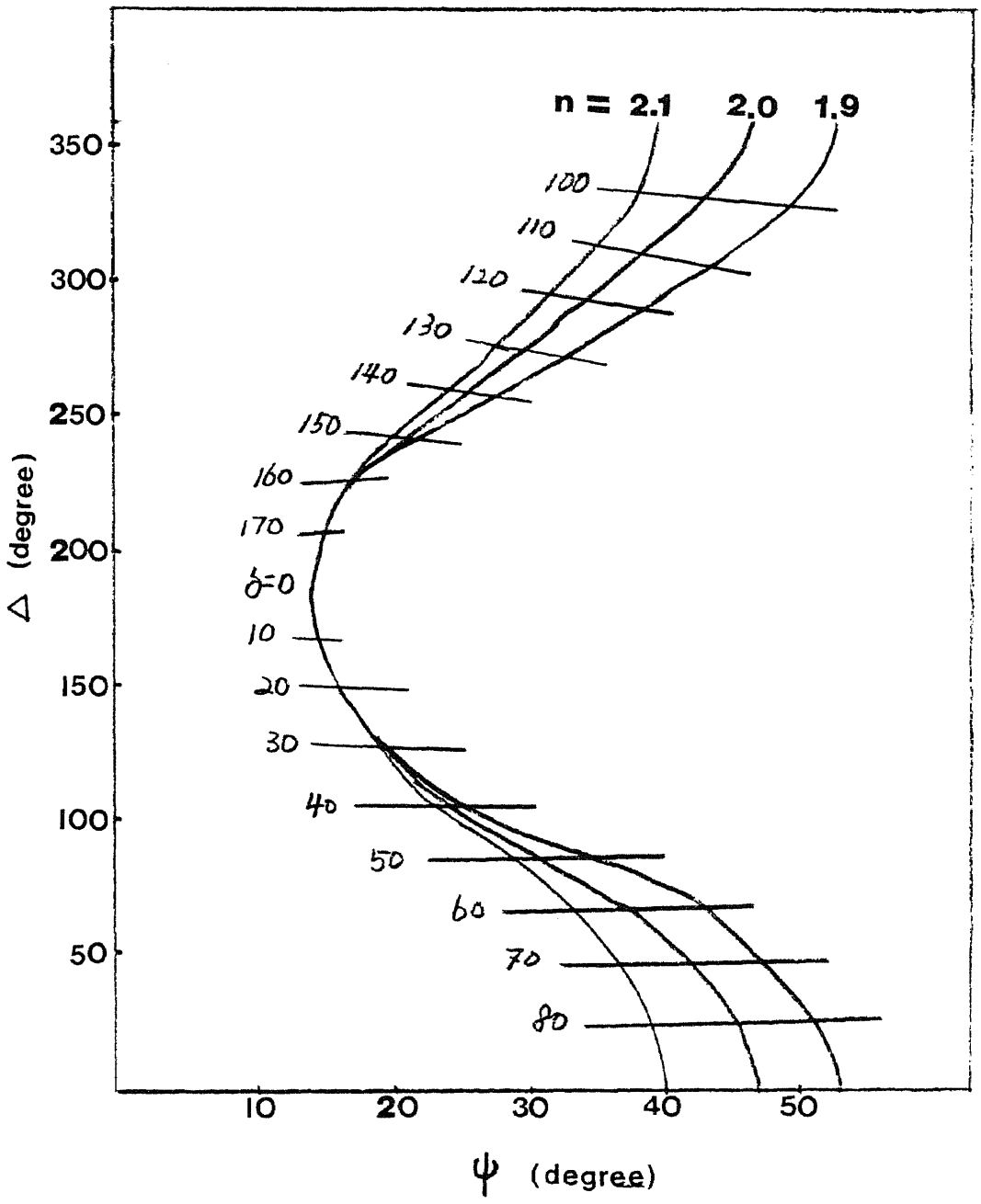

Fig. 3.1

Ellipsometric curves for the Si_3N_4/Si system

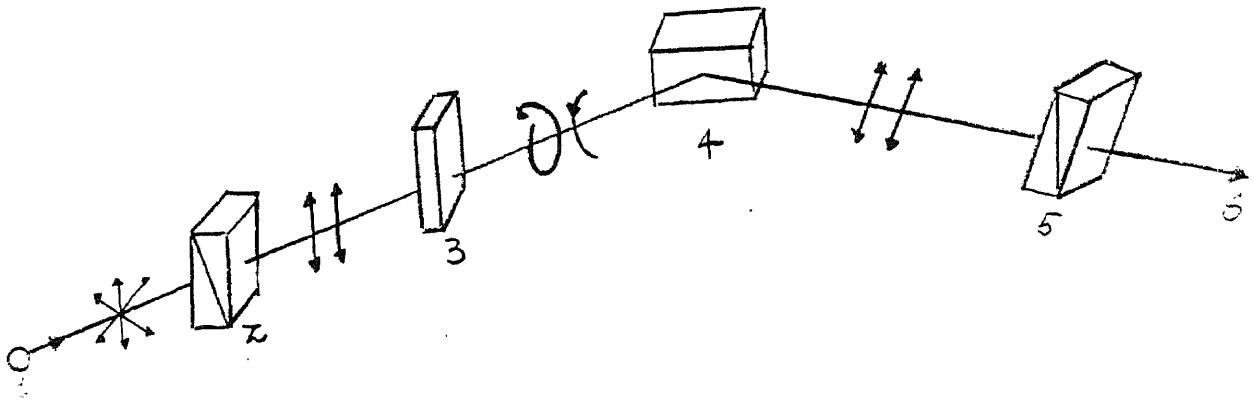

Fig. 3.2

A schematic diagram of an ellipsometer : 1, light source; 2, polarizer; 3, compensator; 4, sample; 5, analyser; 6, detector

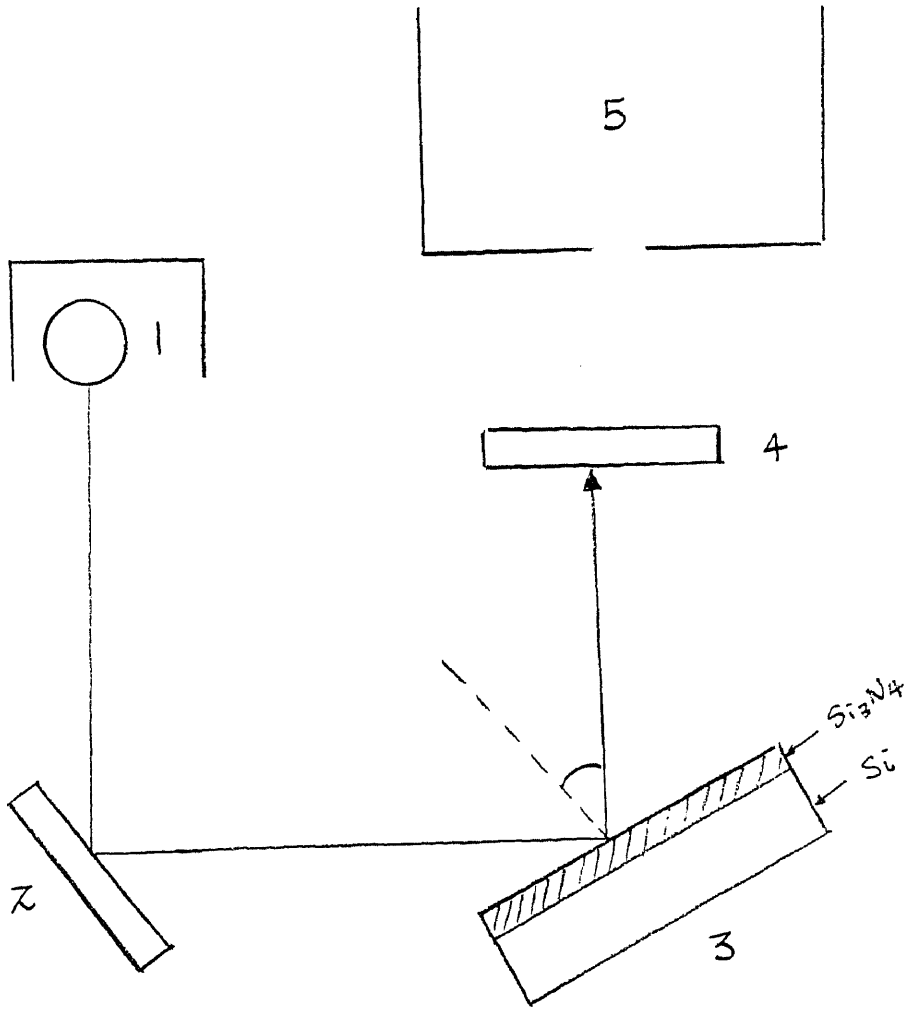

Fig. 3.3

A schematic diagram of the instrument used for measuring film thickness by the VAMFO method: 1, fluorescent lamp; 2, mirror; 3, rotating sample; 4, monochromatic filter; 5, microscope object

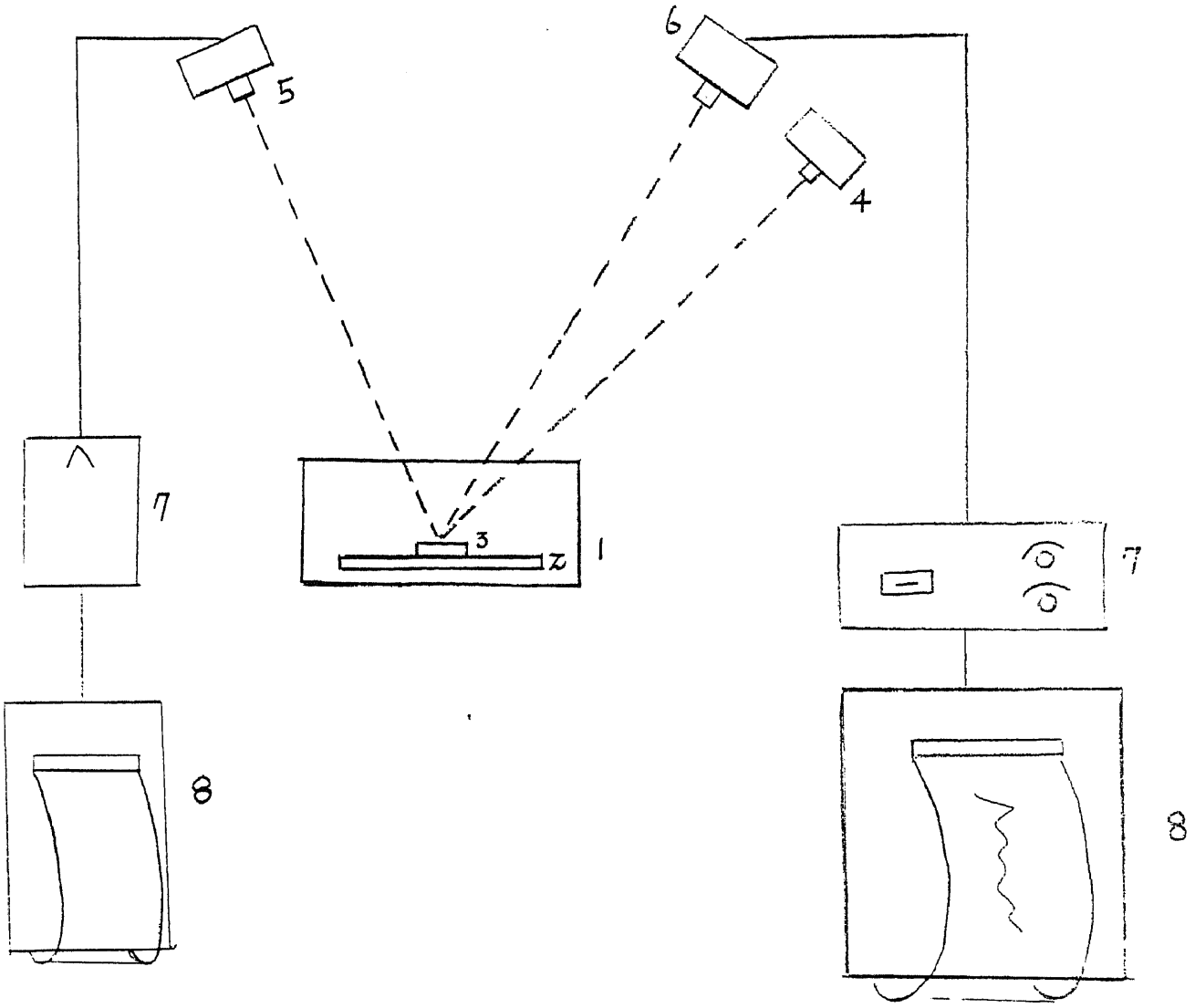

Fig. 3.4

A schematic diagram of in-process film thickness and deposition rate measurement devices: 1, quartz reactor; 2, silicon wafer pedestal; 3, silicon wafer; 4, laser; 5, laser detector; 6, IR detector; 7, amplifiers; 8, strip chart recorders.

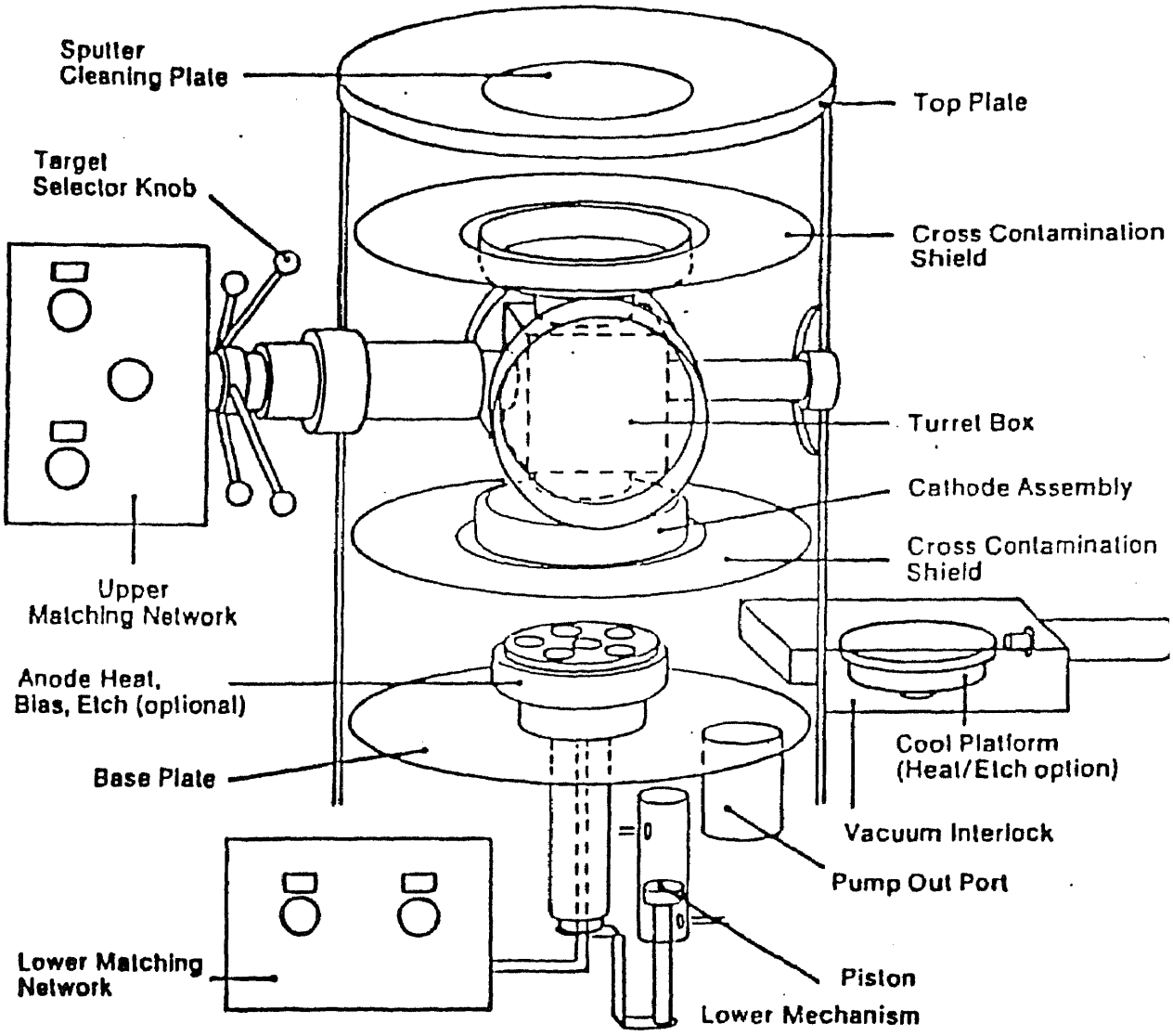

Fig. 4.1 MRC 8800 Sputtering Apparatus

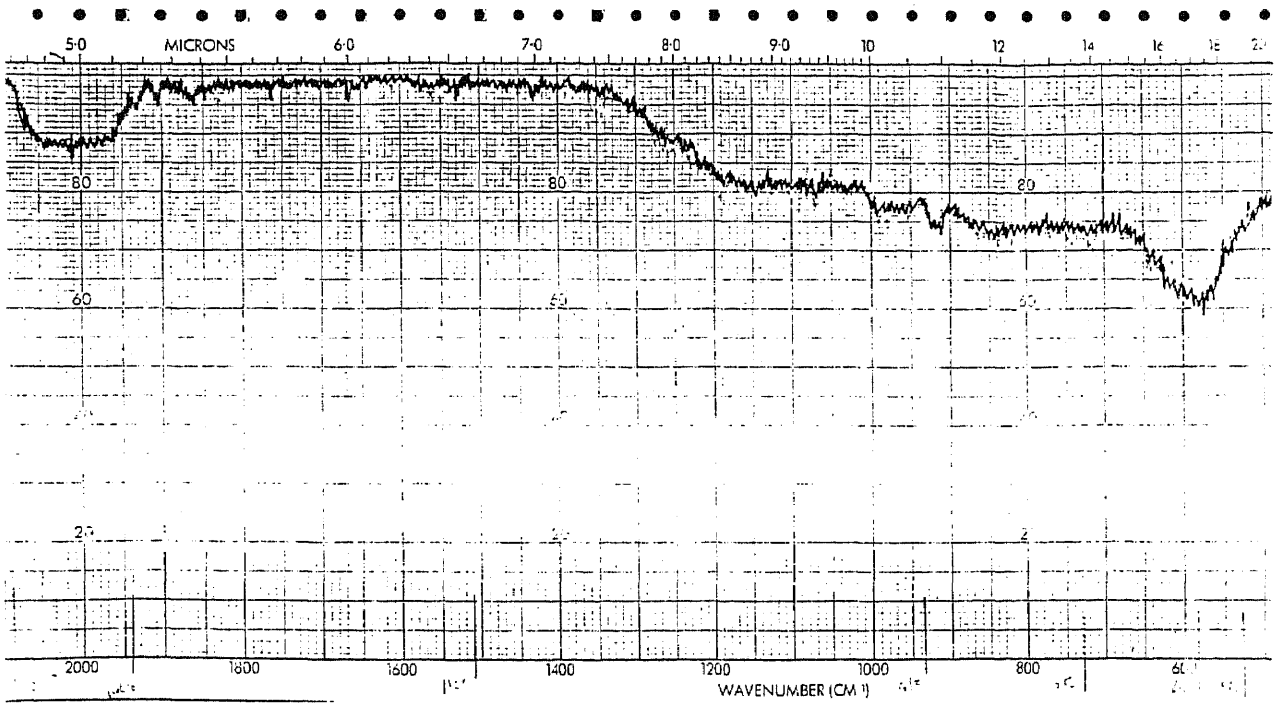

Figure 5.1

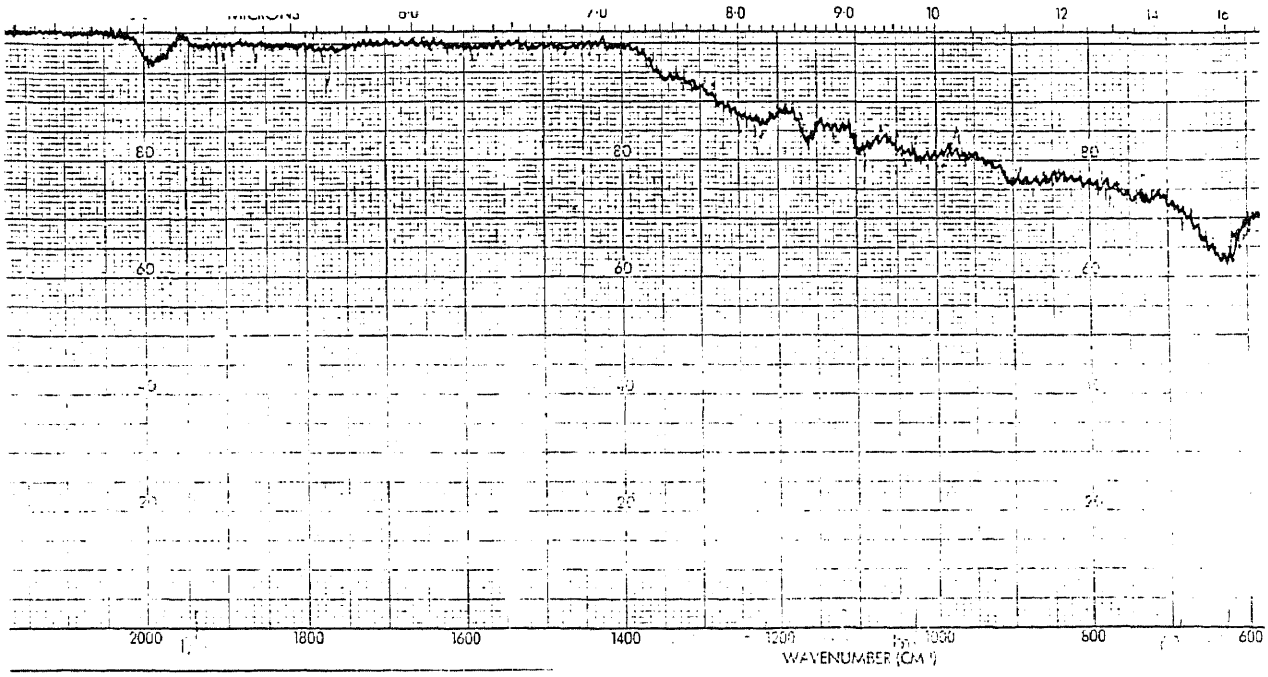

Figure 5.2

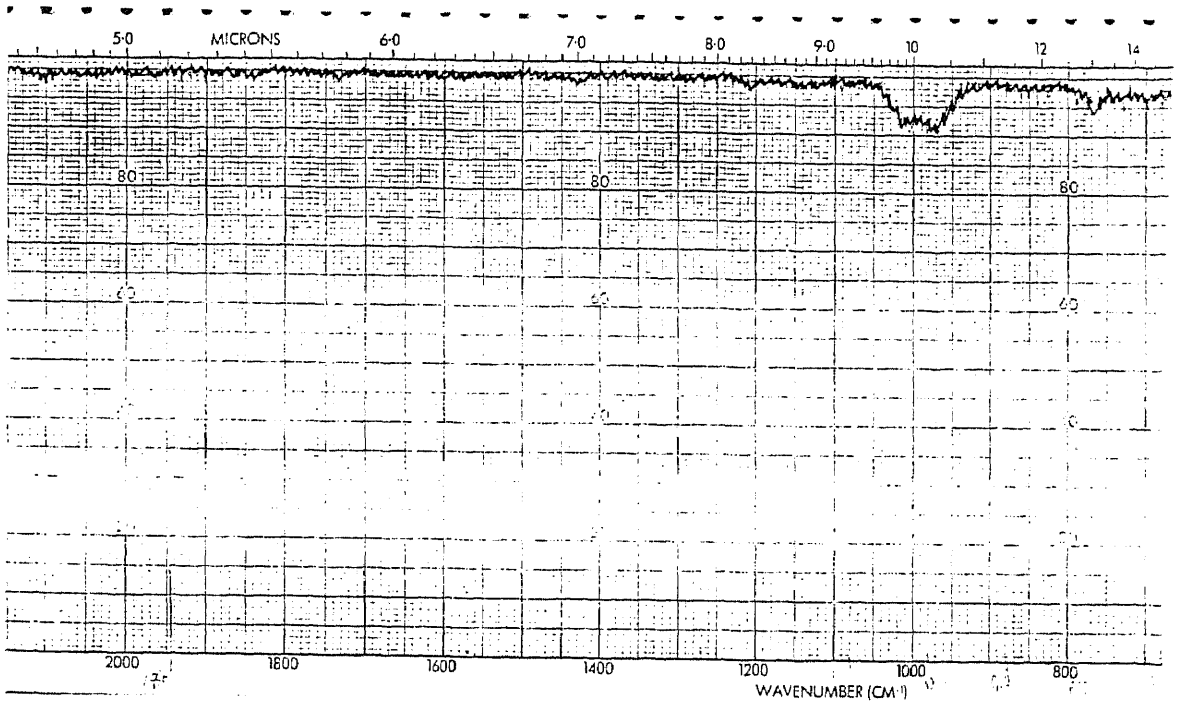

Figure 5.3

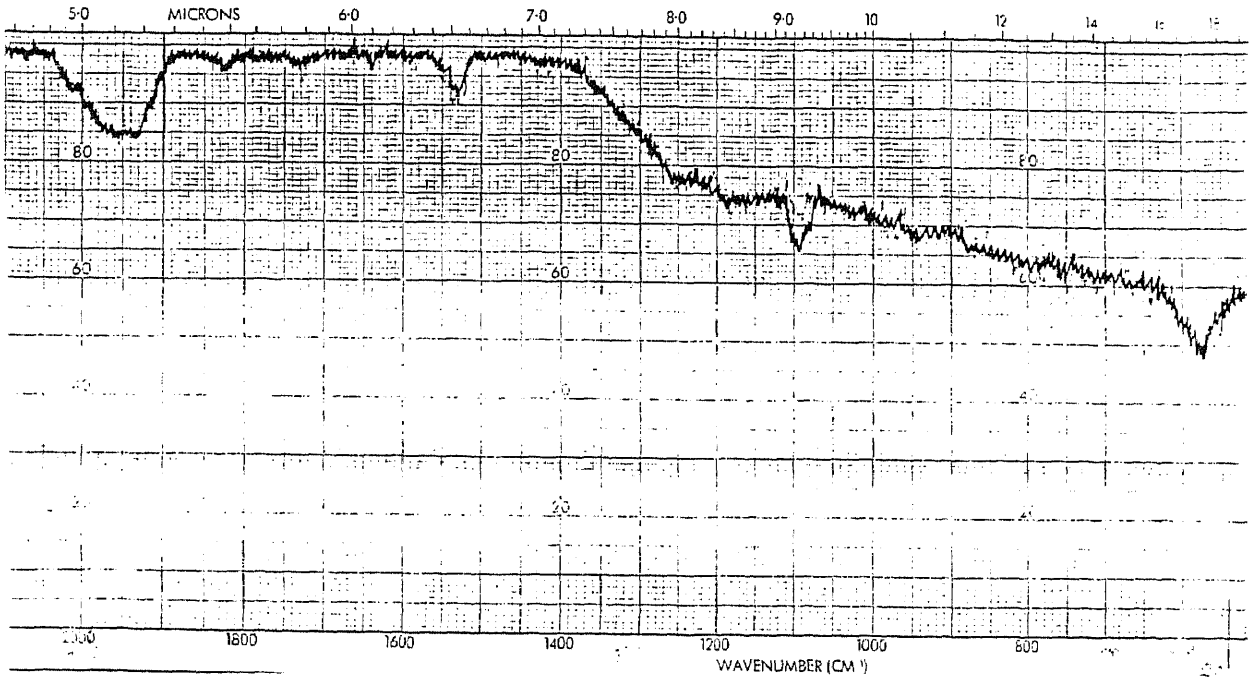

Figure 5.4

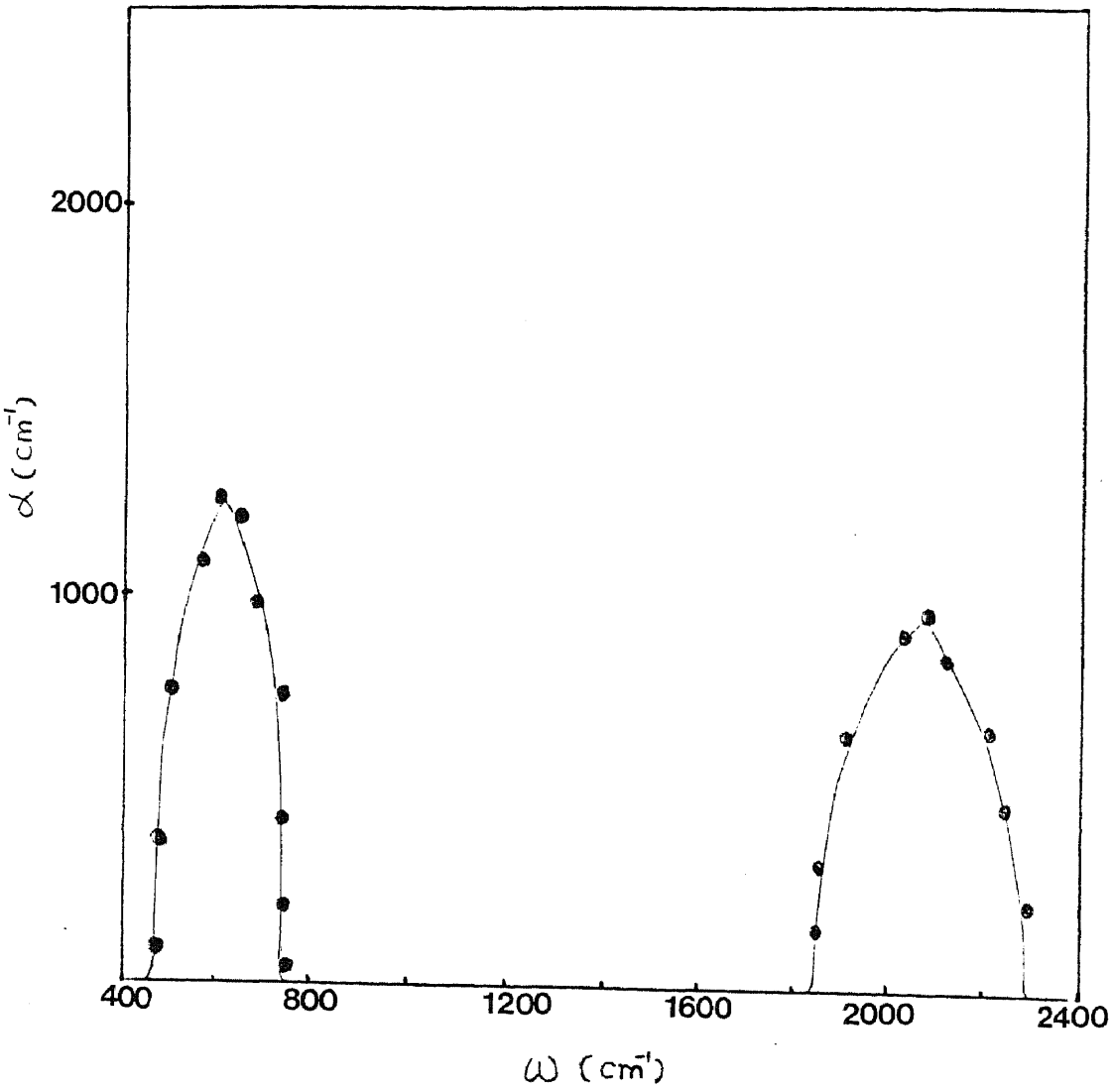

Figure 5.5

Absorption coefficients versus wavenumbers

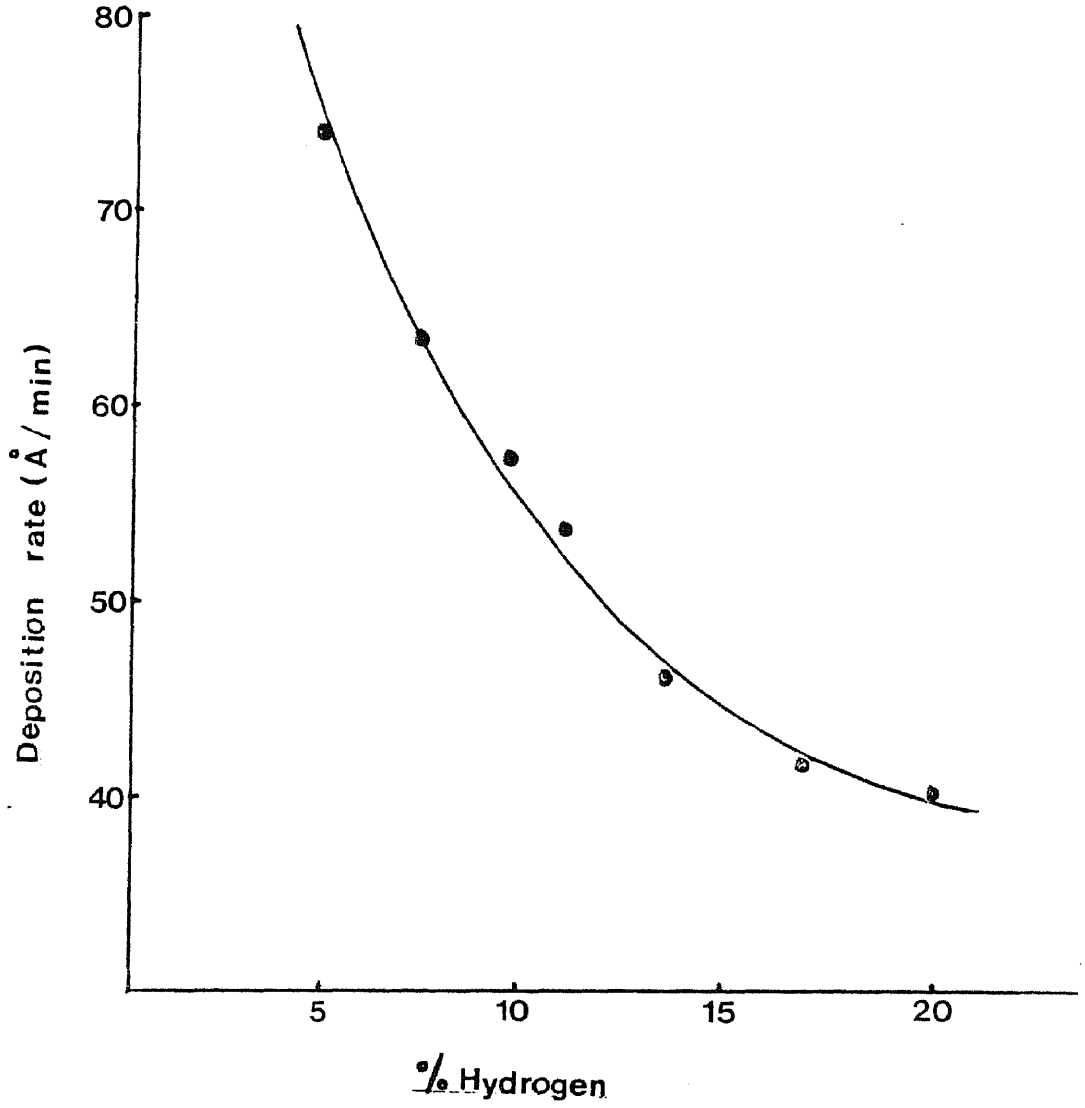

Figure 5.6

Deposition rate versus % hydrogen in vacuum chamber

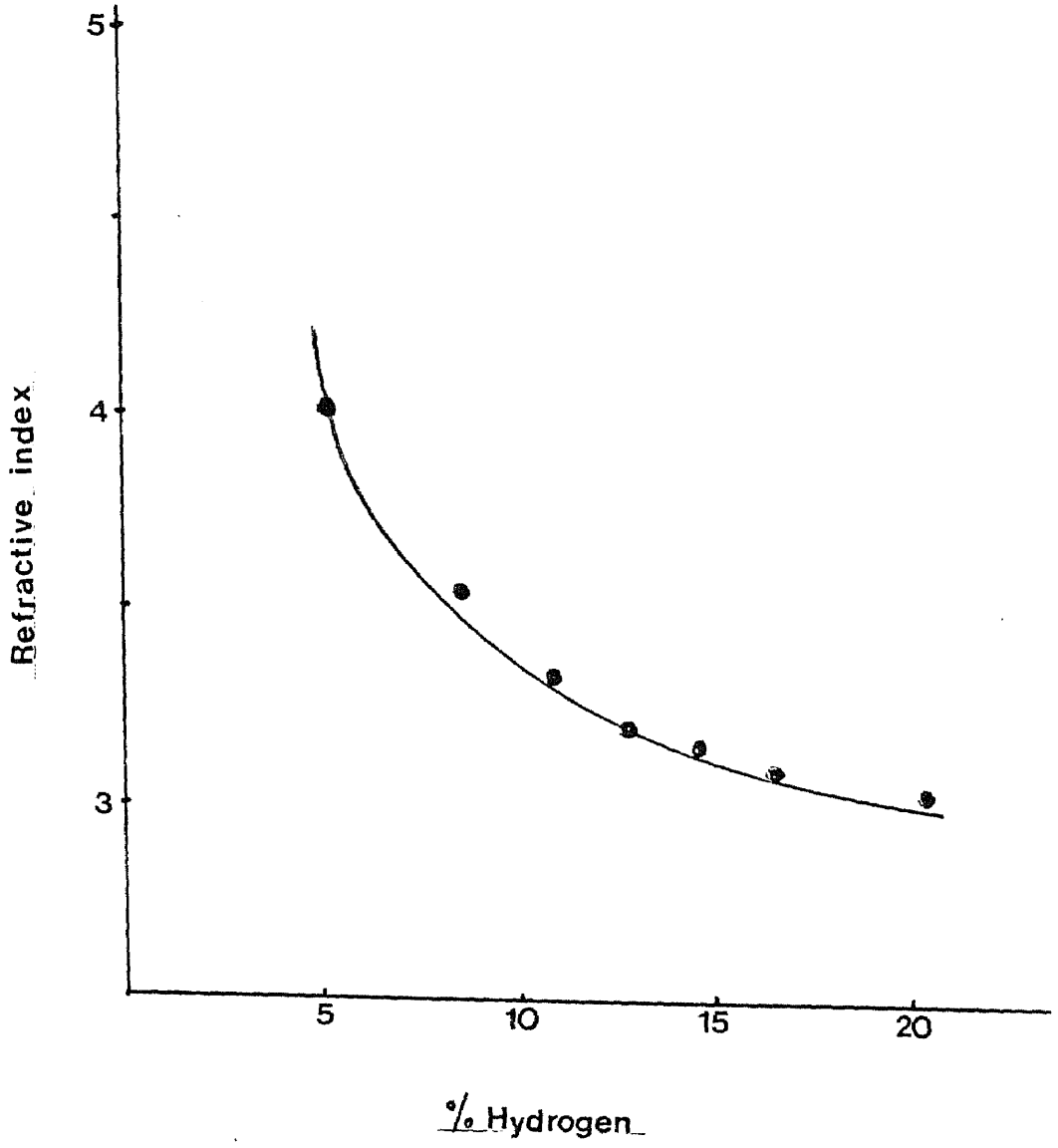

Figure 5.7

Refractive index versus % hydrogen in vacuum chamber

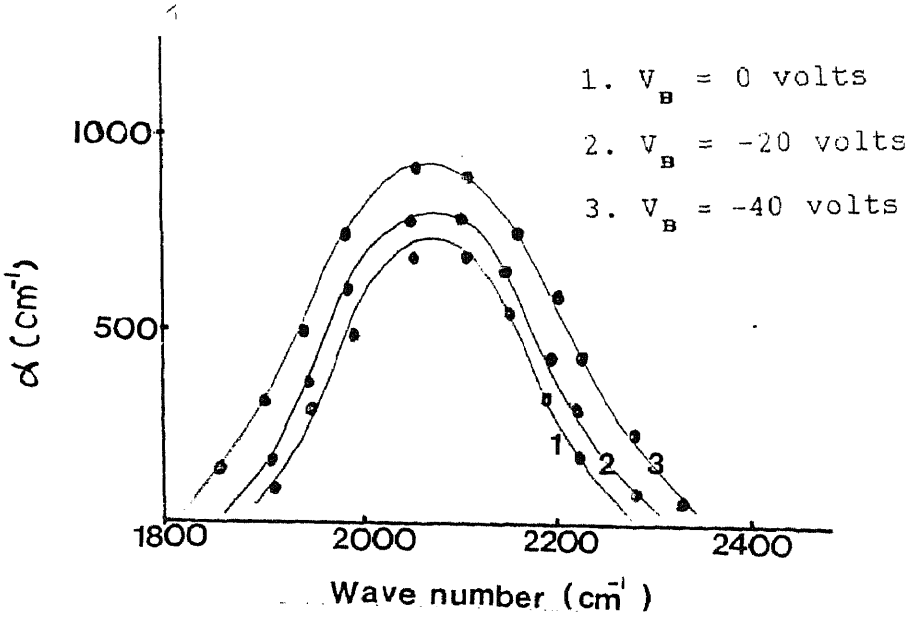

Figure 5.8

Effect of substrate bias on the absorption coefficients of Si-H stretching band at 2000 cm^{-1}

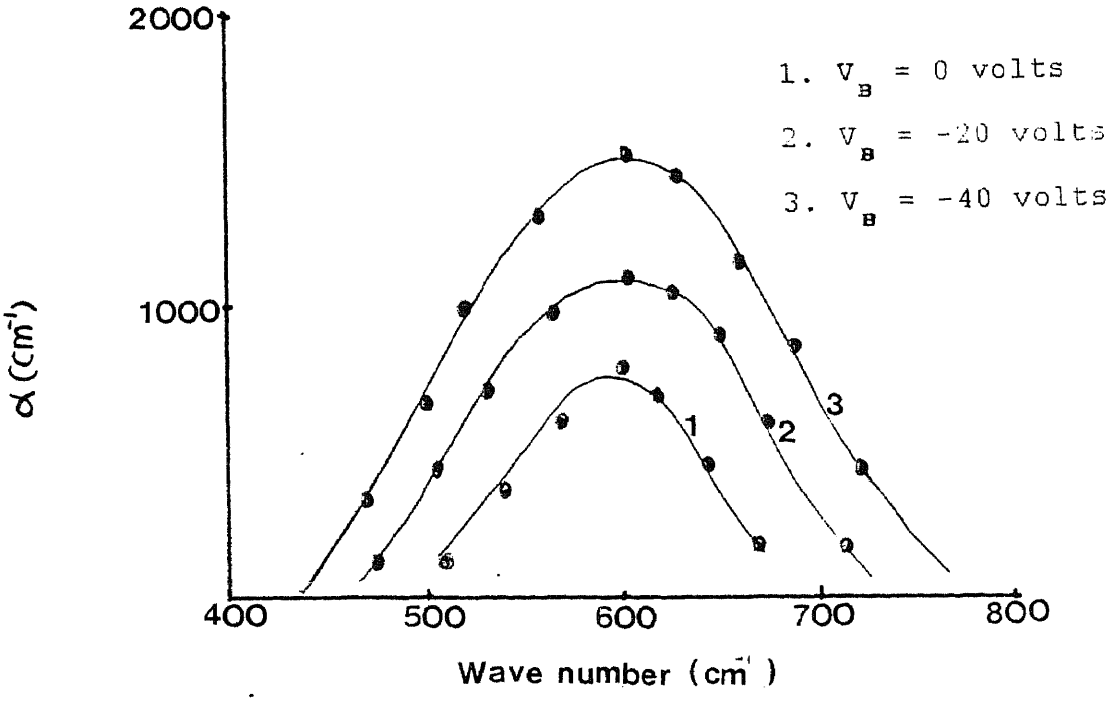

Figure 5.9

Effect of substrate bias on the absorption coefficients of Si-H wagging band at 600 cm^{-1}.

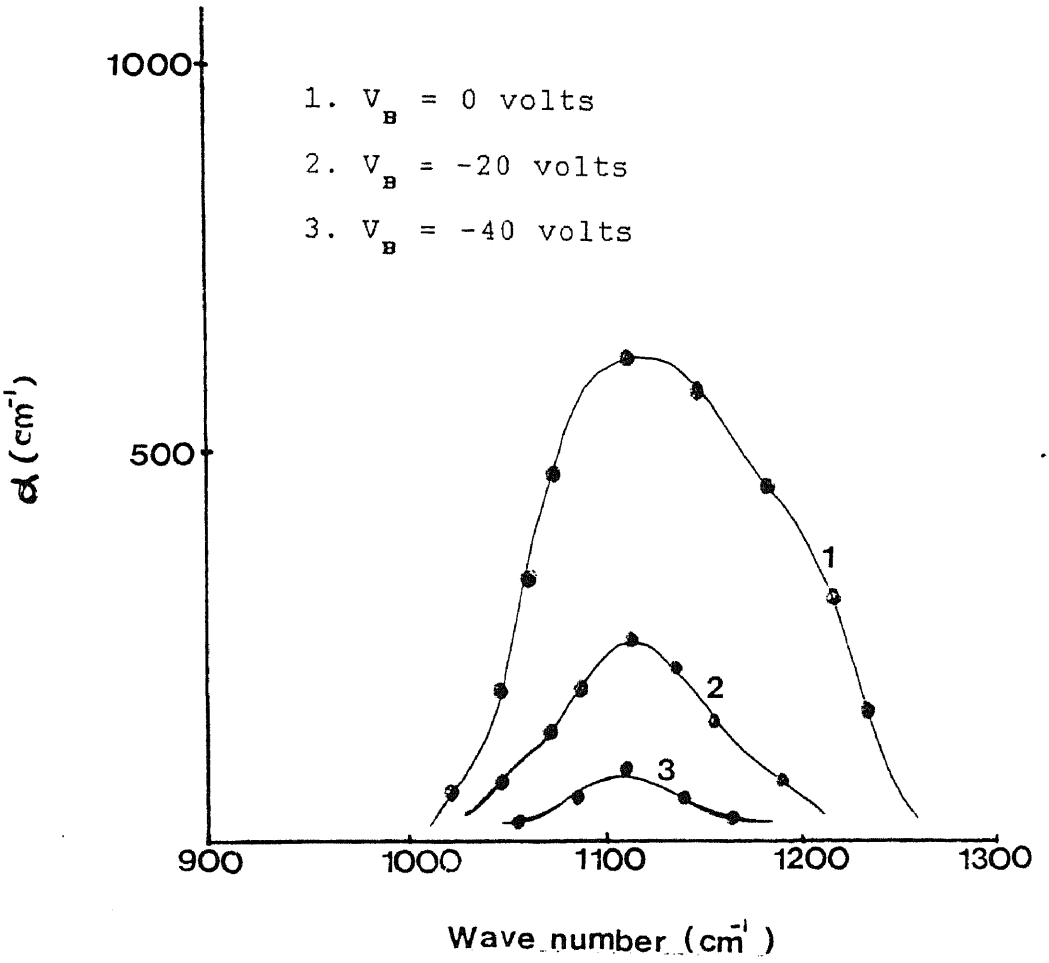

Figure 5.10

Effect of substrate bias on the absorption coefficients of Si-O stretching band at 1100 cm^{-1}.

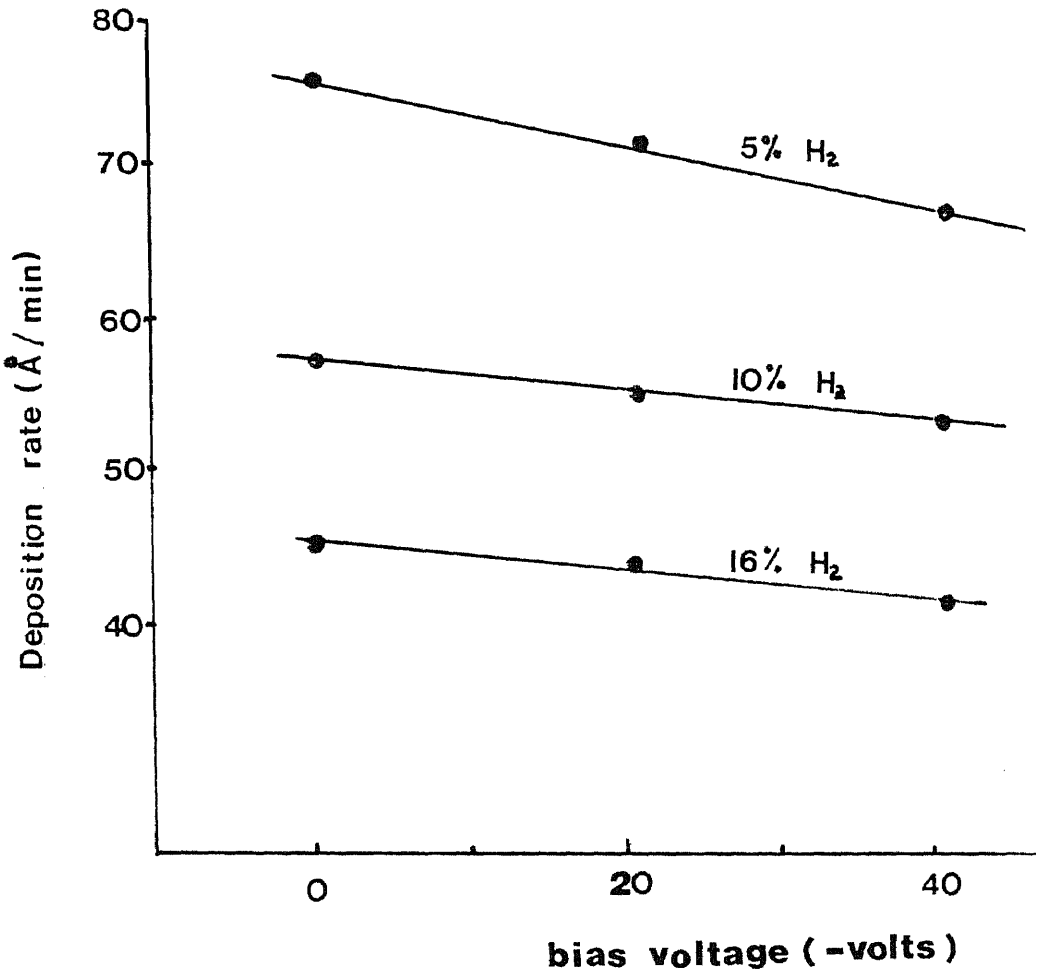

Figure 5.11

Effect of substrate bias on deposition rate

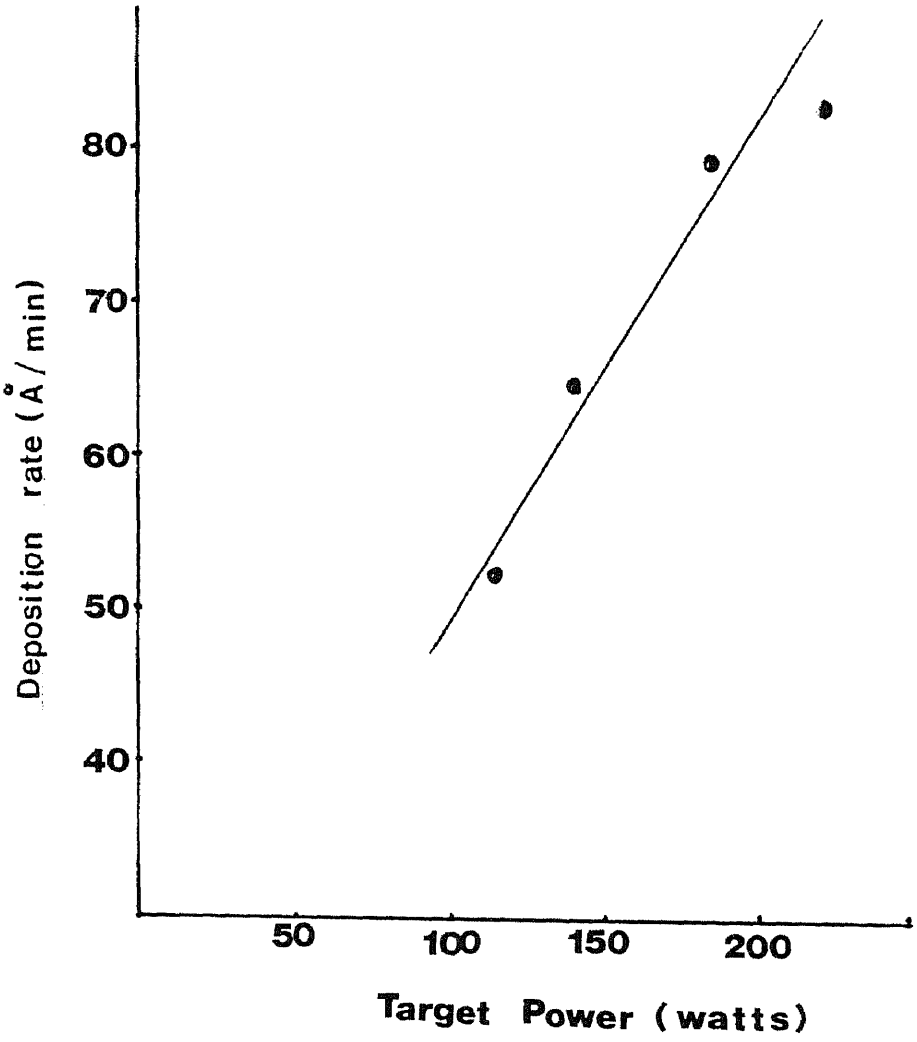

Figure 5.12

Effect of applied target power on deposition rate

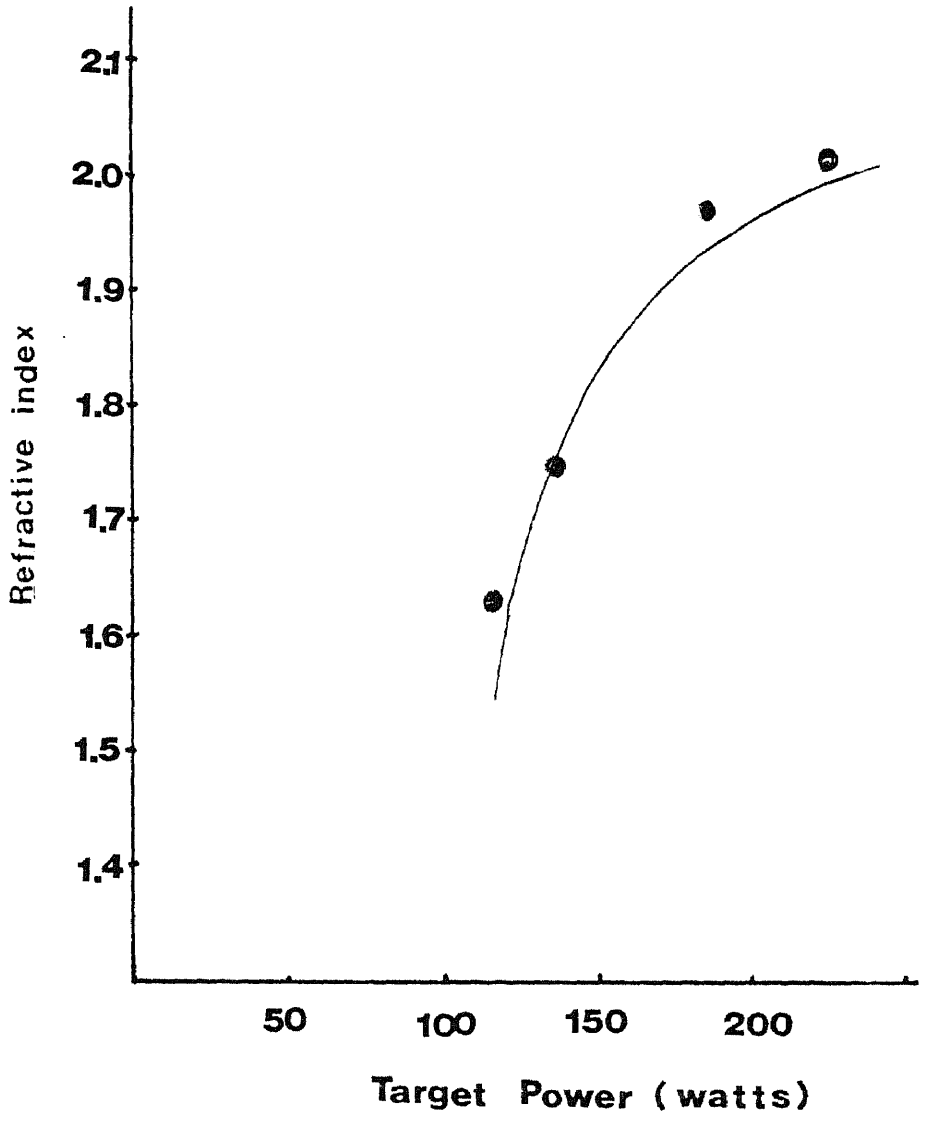

Figure 5.13

Effect of applied target power on refractive index

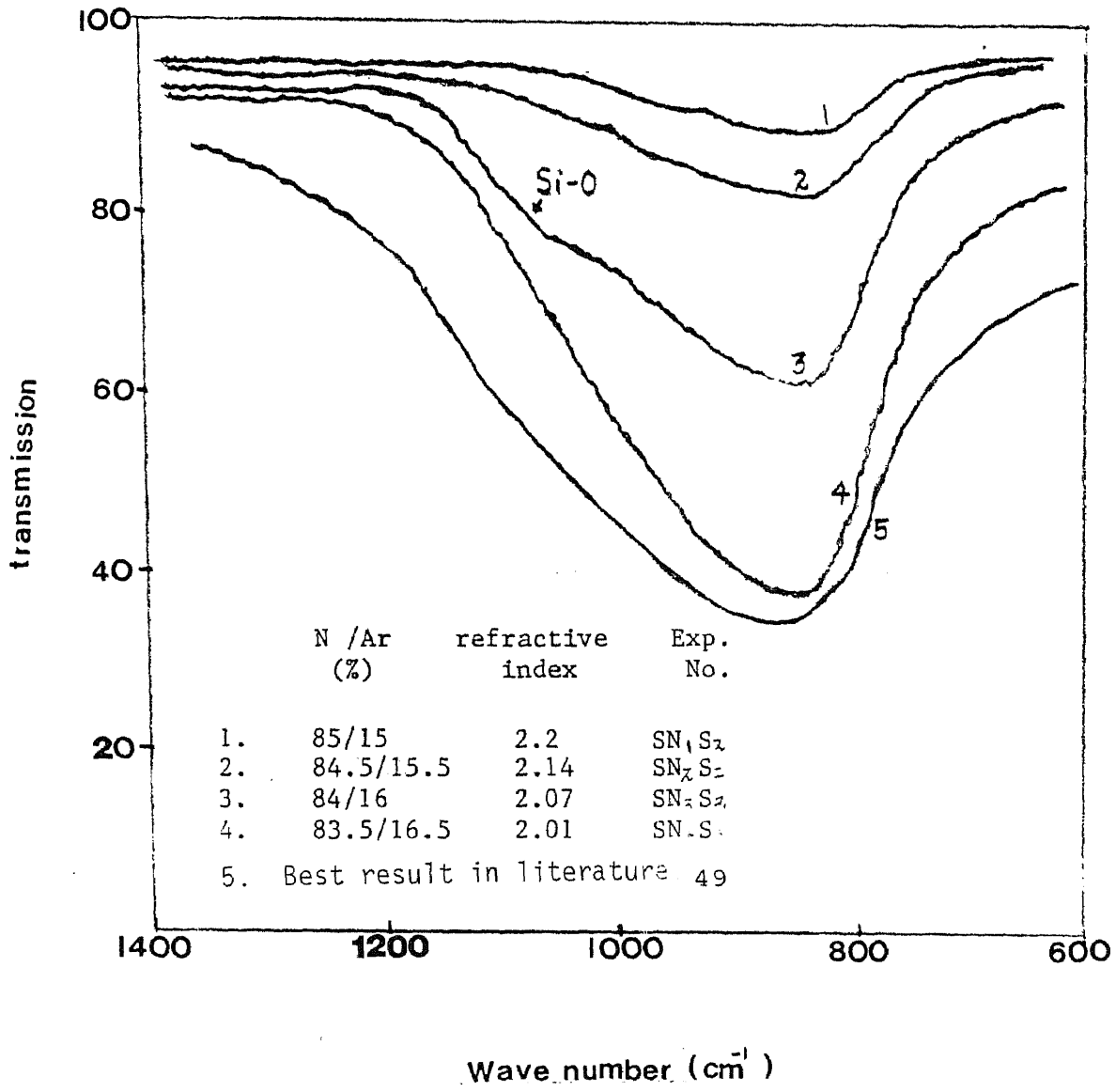

Figure 5.14

Infrared spectra at four different % N_2 content

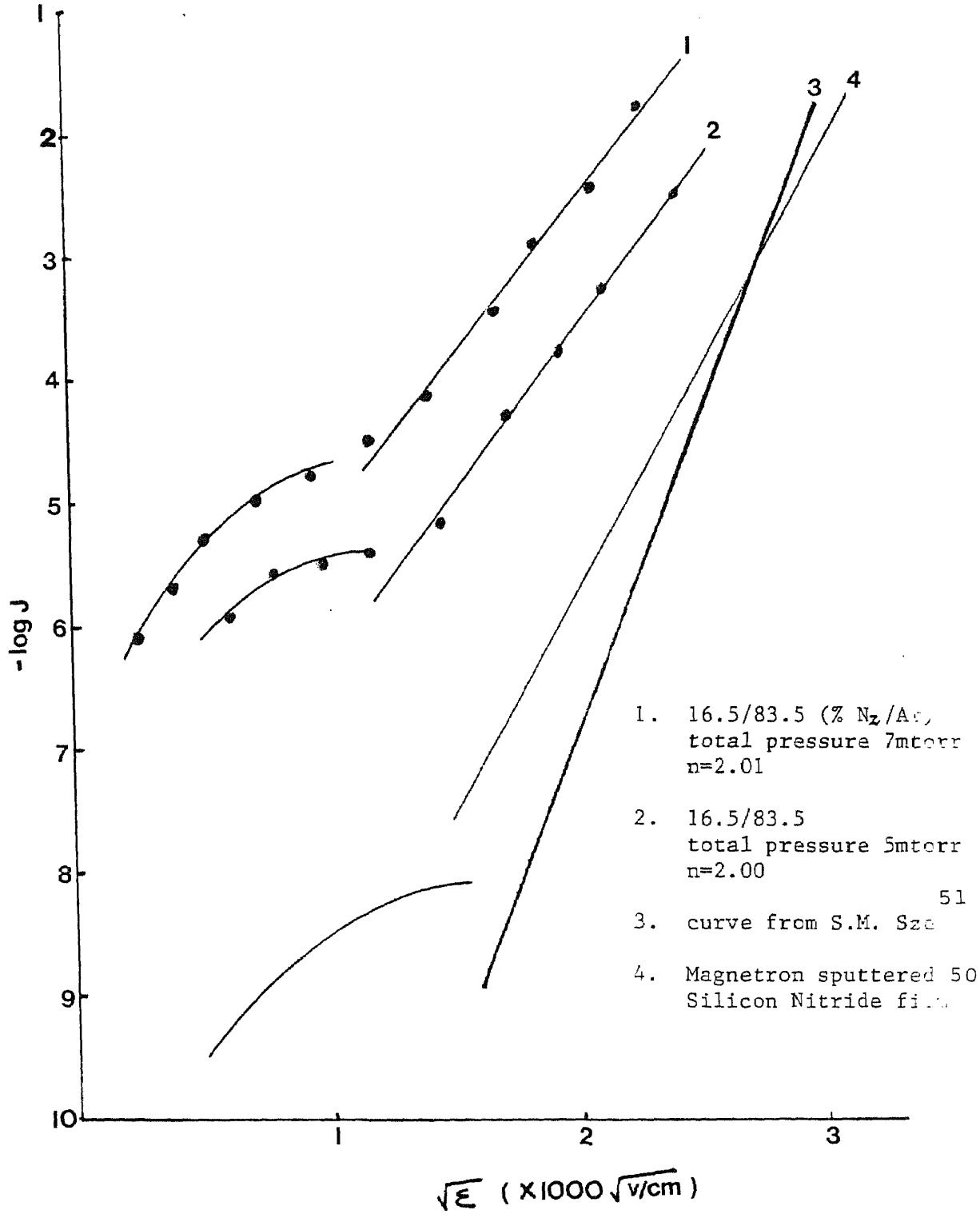

Figure 5.15

Current-voltage curves for MIS capacitor

BIBLIOGRAPHY

1. J.A.Amick, G.L.Schnable, Journal of Vacuum Science and Technology, vol. 14, 1977, pp. 1053.

2. C.E. Morosanu, Thin Solid Films, vol.65, 1980, pp. 171.

3. R.C.G. Swann, R.R. Mehta, Journal of Electrochemical Society, vol.114, 1969, pp. 713.

4. A.K. Sinha, J.J. Levinstein, T.E. Smith, *ibid.*, vol. 125, 1978, pp. 601.

5. E.A. Taft, *ibid.*, vol.118, 1971, pp. 1341.

6. S.M. Hu, L.V. Gregar, *ibid.*, vol.114, 1967, pp. 826.

7. C.M. Drum and M.J. Rand, Journal of Applied Physics, vol. 39, 1968, pp. 4458.

8. E.A. Irene, Journal of Electronic Material, vol. 5, 1976, pp. 287.

9. Y. Misawa and H. Yagi, Japanese Journal of Applied Physics, vol. 16, 1977, pp. 1115.

10. M. Tamura and H. Sunami, ibid., vol.11, 1972, pp. 1097.

11. P. EerNisse, Journal of Applied Physics, vol. 48, 1977, pp. 3337.

12. H.R. Phillip, Journal of Electrochemical Society, vol. 120, 1973, pp. 295.

13. E.A. Lewis, *ibid.*, vol. 111, 1964, pp. 1007.

14. H.J. Stein, Journal of Applied Physics, vol. 47, 1976,

pp. 3421

15. M.J. Rand and D.R. Wonsidler, Journal of Electrochemical Society, vol. 125, 1978, pp. 99

16. S. Go, H. Bilz, and M. Cardona, Physics Review Letter, vol. 34, 1975, pp. 580.

17. D. Wohlheiter, Journal of Electrochemical Society, vol. 122, 1975, pp. 1836.

18. W. van Gelder, and V.E. Hauser, *ibid.*, vol. 114, 1967, pp. 869

19. N.C. Tombs and F.A. Sewell,Jr., *ibid*, vol. 115, 1968, pp. 101.

20. C.A. Deckert, *ibid.*, vol. 125, 1978, pp. 320.

21. K. Sugawara, *ibid.*, vol. 118, 1971, pp. 110.

22. I. Fränz and W. Längheinrich, Solid State Electronics, vol. 14, 1971, pp. 499.

23. C.J. Dell'Oca, Journal of Electrochemical Society, vol. 120, 1973, pp. 1225.

24. T.B. Tripp, *ibid.*, vol. 117, 1970, pp. 157.

25. B.E. Deal, P.J. Flemming, and P.L. Castro, *ibid.*, vol. 115, 1968, pp. 300.

26. G.A. Brown, H.G. Carlson, *ibid.*, vol. 115, 1968, pp. 273.

27. C.A. Barile, R.C. Dockerty and A. Nagarajan, *ibid.*, vol. 121, 1974, pp. 907.

28. M. Maekawa, Japanese Journal of Applied Physics, vol. 11, 1972, pp. 1251.

29. J.R. Cricchi and D.F. Barbe, Applied Physic Letter, vol. 19, 1971, pp. 49.

30. P.C. Arnett and D.J. Di Maria, *ibid.*, vol. 27, 1975, pp. 34.

31. S.M. Sze, Journal of Applied Physics, vol. 38, 1967, pp. 2951.

32. D. Frohman-Bentchkowsky and M. Lenzlinger, *ibid.*, vol. 40, 1969, pp. 3307.

33. E.J.M. Kendall, *ibid.*, vol. 46, 1973, pp. 2509.

34. E.J.M. Kendall, *ibid.*, vol. 48, 1974, pp. 1409.

35. Z.A. Weinberg and R.A. Pollak, Applied Physic Letter, vol. 27, 1975, pp. 254.

36. B.H. Yun, *ibid.*, vol. 27, 1975, pp. 256.

37. W. Stutins and W. Streifer, Applied Optics, vol. 16, 1977, pp. 3218.

38. H. Ogawa, T. Nishinaga, M. Kasuga and T. Arizumi, Japanese Journal of Applied Physics, vol. 10, 1971, pp. 1975.

39. N.P. Chou, J.A. Aboaf, Applied Physics Letter, vol. 27, 1975, pp. 356.

40. K. Niihara and T. Hirai, Journal of Material Science, vol. 12, 1977, pp. 1233.

41. B.J. Sealy and J.M. Ritchie, Thin Solid Films, vol. 35, 1976, pp. 127.

42. J.P. McCloskey, Journal of Electrochemical Society, vol. 114, 1967, pp. 643.

114, 1967, pp. 643.

43. M.H. Brodsky, M. Cardona and J.J. Cuomo, Physical Review, vol. 16, no. 8, 1977, pp. 3556.

44. J. Tardy and R. Meaudre, *ibid.*, vol. 13, 1976, pp. 787.

45. A.K. Ghosh, T. McMahon, E. Rock, and H. Wiesmann, Journal of Applied Physics, vol. 50, 1979, pp. 3407.

46. J. Anderson, P. Moddel, M. Paesler and K. Paul, *ibid.*, vol. 48, 1977, pp. 5227.

47. S.M. Hu, L.V. Gregor, Journal of Electrochemical Society, vol. 114, 1967, pp. 826.

48. Y. Kuwano, Japan Journal of Applied Physics, vol. 8, 1969, pp. 876.

49. M. Shiloh, Journal of Electrochemical Society, vol. 124, 1977, pp. 295.

50. T. Serikawa and A. Okamoto, *ibid.*, vol. 131, 1984, pp. 2928.

51. S.M. Sze, Journal of Applied Physics, vol. 38, no. 7, 1967, pp. 2951.